

# Journal of the Geological Society

## Alluvial fan shifts and stream captures driven by extensional tectonics in central Italy --Manuscript Draft--

<b>Manuscript Number:</b>	jgs2017-138R2
<b>Article Type:</b>	Research article
<b>Full Title:</b>	Alluvial fan shifts and stream captures driven by extensional tectonics in central Italy
<b>Short Title:</b>	Extension modifies alluvial fans and rivers
<b>Corresponding Author:</b>	Francesco Mirabella Universita degli Studi di Perugia Dipartimento di Fisica e Geologia ITALY
<b>Corresponding Author E-Mail:</b>	francesco.mirabella@unipg.it
<b>Other Authors:</b>	Francesco Bucci Michele Santangelo Mauro Cardinali Grazia Caielli Roberto De Franco Fausto Guzzetti Massimiliano Rinaldo Barchi
<b>Manuscript Classifications:</b>	Geohazards; Geomorphology; Tectonics
<b>Additional Information:</b>	
<b>Question</b>	<b>Response</b>
Are there any conflicting interests, financial or otherwise?	No
Samples used for data or illustrations in this article have been collected in a responsible manner	Confirmed
<b>Response to Reviewers:</b>	

Perugia May 22<sup>nd</sup>, 2018

Dear Editor,

Please find enclosed the revised version of manuscript No. jgs2017-138R1, “Alluvial fan shifts and stream captures driven by extensional tectonics in central Italy”, submitted for publication in the Journal of the Geological Society.

Following your indication on our revised version R1 to shorten the text, we significantly reduced the text in the figure captions. Besides, we also simplified some sentences in the main text and we erased duplications.

We shortened the text by over 1.000 words without losing important details. We hope this reduction is enough to make the manuscript fit the Journal.

Finally we re-numbered the figures.

We enclose:

- **a revised clean version of the manuscript**
- **a revised version of the manuscript with visible changes**
- **a separated file containing only the figure captions with the changes made**

We believe the text now reads much better and we hope to hear from you soon.

Sincerely,  
Francesco Mirabella

## Manuscript jgs2017\_138R1 – Changes to Figure captions

### Figure captions

**Fig. 1.** (a) Location map of the study area. The map shows the position of the historical seismicity ( $M \geq 5$ ), of the main normal faults and the position of the present-day alluvial-fans and alluvial deposits. The map also reports a sketch of the underlying geology. (b) **Study** area within the main normal faults alignment from Spoleto to the SE to Sansepolcro to the NW.

**Fig. 2.** (a) Geological sketch of the area across the Bastardo and Foligno valleys. The sketch is oriented SW-NE and is redrawn from- and integrated with- the map after Bucci et al. (2016a). ~~The map shows the geometry of the incised Bastardo valley to the SW, the geometry of the Foligno valley present-day alluvial plain to the NE and the position of a remnant of the Montefalco unit east of Foligno.~~ The map reports the traces of the high resolution seismic reflection profiles (Fig.5a, b) and the trace of the integrated geological cross-section (A-A', Fig.5c). (b) Sketch of the stratigraphic relationships within the area. ~~See text for stratigraphy details. The Bastardo valley (to the SW) is mainly infilled with an Early-Middle Pleistocene continental sequence. The Foligno valley (to the NE) is almost entirely occupied by a thick alluvial deposit sequence and by alluvial fans mostly delivering sediments from the NE.~~

**Fig. 3.** (a) View towards the East of the Foligno fan from the Montefalco hill. The rose-diagram reports the palaeo-currents indicators of the Montefalco alluvial fan. The diagram is the sum (red line) of the data ( $n = 34$ ) acquired by Regione Umbria (2014) (blue line) and of the data ( $n = 32$ ) within this work (green line). Inset a) also reports the position of the outcrops of insets 3c and 3d. (b) Example of embricate clasts in the Montefalco Unit composed of organised in layers. The stereographic projection reports the poles ( $n = 28$ ) of bedding layers (yellow), the dip direction (blue) of embricate planes ( $n = 32$ ), and the computed flow direction (blue arrow). (c) **Outcrop of the wWell** cemented embricate clasts of the Montefalco Unit. The position of the outcrop is **reported in the** Fig. 3a). (d) Outcrop of the Montefalco Unit at Foligno (outcrop position in Fig. 3a). Here, the facies is more proximal (**with larger and poorly embricate clasts**) than at Montefalco (**outcrops in** Figs. 3b and 3c).

**Fig. 4.** (a) View towards the South of the Montefalco hill, showing the sub-horizontal beds (yellow) and the morphological evidence of the NE-dipping normal faults. The stereo-plot is the stereographic projection (Schmidt net, lower hemisphere) of the mapped normal faults ( $n = 7$ ) and the resulting stresses analysis. (b) Outcrop of a normal fault (**outcrop** position in a) within the continental sequence and fault kinematics. (c) View of the western part of the Bastardo valley (filled by the Colle del Marchese Unit – CU, and the Bevagna Unit - BU), at the contact with the Mt. Martani ridge (shaped on the Bedrock). The stereographic projection (Schmidt net, lower hemisphere) reports poles to planes ( $n = 27$ ) of the Giano dell'Umbria Fault system and the resulting average dip and kinematics (red arrow). (d) **Outcrop Geometry and kinematics of one of the faults of the Giano dell'Umbria fault System (outcrop-position in c) with geometry and kinematics.**

**Fig. 5.** (a-b) High resolution seismic reflection profiles (trace in figure 2a) showing the ~~The seismic profiles show the~~ depth geometry of the Bevagna Unit, of the normal faults bordering the eastern flank of the Montefalco hill and the thickness of the alluvial deposits. (a) Shows the difference in seismic facies between the bedrock at the normal faults footwall and the layered continental sequence made of sands and clays. (b) **Shows that the SW-tilt of the** Bevagna Unit and **is tilted to the SW towards the normal faults and that the** alluvial deposits thickening towards the SW. (c) Geological cross-section (trace in figure 2) across the Foligno valley which integrates the surface geology and the seismic profiles of a) and b). The SW part of the section is extrapolated

to depth of the basis of a) and b), the NE part of the section is extrapolated to depth on the basis of previous work (Barchi et al., 1991). The section reaches the outcrop of the Montefalco Unit near Foligno (locality "I Cappuccini", Fig.2a).

**Fig. 6.** Geomorphological map of the study area. The map is oriented E-W and shows the evidences of drainage perturbation on both the western and eastern reliefs induced by the increase in subsidence of the Foligno valley. The numbers refer to the drainage areas of specific rivers **which captured of were captured by a nearby river. for which we identify evidences of capturing or which underwent capture by a nearby river**. The numbers are the same as those in figure 7. We mapped the geomorphological anomalies related to the migration of the watershed, hanging palaeo-valleys, anomalous confluences and the direction of the palaeo-rivers for the most significant rivers in the study area. See text for description and discussion.

**Fig. 7. (a)** Log-Log plot of the alluvial fans areas towards basins areas of the study area. The regression line was obtained through a logarithmic space quantile regression, applied to the 50<sup>th</sup> (dotted thick line) 5<sup>th</sup>, and 95<sup>th</sup> percentiles (grey shaded area) of the distribution. **The plot shows a roughly self-similar. The data distribution is self-similar of data** (equation of the type  $A_F = q * A_B^n$ ). **(b)** Distribution of the alluvial fans (points in Figure 7a) related to **capturing and captured rivers which either captured or underwent capturing**. In both figures, red and black numbered circles represent the alluvial fans related to rivers clearly perturbed by the Foligno valley subsidence which induced captures and drainage inversions (Figure 6).

**Fig. 8. (a)** stream-long profiles of the Mauro, La Fornace and La Torre streams plotted together with the downstream variation in slope % ( $dH/dL$ , where H is elevation and L is distance). The symbols (diamond, circle, triangle, square and star) represent the correspondence between stream knick-points and mapped normal faults. **(b)** map location (inset of in Fig. 2) of the streams shown in a) on the NE-flank of the Montefalco hill. **(c)** drape of an aerial photograph on a 10m resolution DEM (TIN-Italy - Tarquini et al., 2007). We used a three-times vertical exaggeration to mimic the vertical exaggeration of the stereoscopic images. The image was drawn by using the QGIS2threejs plugin of QGIS (QGIS Development Team, 2018). On the image, the trace of the normal fault affecting the Holocene alluvial fans is evidenced with the white arrows.

**Fig. 9.** Tectono-sedimentary evolution of the study area. ~~The units names and acronyms are the same as in figure 2.~~ **(a) Early-Middle Pleistocene, initial formation of the continental basin. the basin bounding normal faults produced active subsidence of the basin, the deposition of the Bevagna Unit and of the Montefalco Unit. In the W part of the basin (Bastardo valley), the Colle del Marchese Unit was also being deposited by the palaeo-Torinetto and palaeo-Rovicciano streams. During this stage the Puglia river was flowing to the SE into the Bastardo valley and the Menotre river was still flowing to the SW into the Foligno valley and the watersheds were still following the alignment of the highest elevations. (b) Middle-Late Pleistocene, the increase in activity of the Montefalco east-dipping faults which presently border the Montefalco hill to the east downthrows the Foligno valley and uplifted the Montefalco alluvial fan de-activating it. The Bastardo valley remained active as an endorheic basin where the Pianacce Unit deposited. The event also produced a complete re-organization of the rivers network and triggered headward erosion of the Attone, Topino and Menotre rivers. The palaeo-Rovicciano stream was diverted from its original NE direction towards the Foligno valley to the SE. (c) Upper Pleistocene-Holocene, the last stage is the further downthrowing of the Foligno valley produced a and strong enhanced-stream headward erosion. See test for details, development of stream piracy. This erosional event was strong enough to break the thresholds and allowed both the Puglia and the Attone rivers to enter the Bastardo valley and incise the Pianacce Unit. As a result the present-day watershed is located in the middle of the Bastardo**

valley. Headward erosion of the Topino river reached the catchments of the palaeo-Menotre river inverting it.

**Fig. 10.** Conceptual sketch of the growth of a set of alluvial fans in an actively subsiding basin where one or more fault segments are more active than others. **Increase of tectonic subsidence triggers headward erosion and drainage capture of neighboring rivers.** See text for explanation. ~~Stage 1 represents three alluvial fans and their catchments draining the footwall of oppositely dipping normal faults into a basin. If one fault is more active than the others, the catchment of alluvial fan B will increase its headward erosion to re-equilibrate with respect to the increased subsidence of its relative base level. At this stage, on a plot of fan area vs basin area, all the three fans will lie on a common regression line between the two parameters. At Stage 2, as subsidence increases, headward erosion of the rivers of fan B can be so efficient to break the threshold with the catchment of the nearby river delivering sediments to fan C and cause drainage capture and inversion of the C catchment. In a plot of fan area vs basin area this stage is marked by the migration of the capturing river basin area and by a decrease of the basin area of the captured river. This process is relatively fast and at this stage the fans areas have not yet enough time to re-adjust their size with respect to the modification underwent by their draining areas. At stage 3, re-equilibration occurs as the captured river will rapidly increase its fan size in response to the increase of its catchment. At the same time the captured river will possess a fan which is too large compared to its reduced catchment.~~

# Alluvial fan shifts and stream captures driven by extensional tectonics in central Italy

Mirabella Francesco <sup>1\*</sup>, Bucci Francesco <sup>2</sup>, Santangelo Michele <sup>2</sup>, Cardinali Mauro <sup>2</sup>, Caielli Grazia <sup>3</sup>; De  
Franco Roberto <sup>3</sup>; Guzzetti Fausto <sup>2</sup> & Barchi Massimiliano R. <sup>1</sup>

<sup>1</sup> *Dipartimento di Fisica e Geologia, Università degli Studi di Perugia, Italy*

<sup>2</sup> *CNR, Istituto di Ricerca per la Protezione Idrogeologica nell'Italia Centrale, via della Madonna Alta 126,  
06128 Perugia, Italy*

<sup>3</sup> *CNR Istituto per la Dinamica dei Processi Ambientali, via Mario Bianco 9, 20131 Milano, Italy*

\* *Corresponding author (email: francesco.mirabella@unipg.it)*

**Abstract:** Subsidence of a normal fault bounded basin in central Italy in the last 0.78 Myr caused the deactivation and uplift of an Early-Middle Pleistocene alluvial fan at the fault footwall. Uplift of the fan occurred with a basin-bounding fault slip-rate in the order of 0.2 mm/yr. Subsidence produced the re-organization of the rivers network due to base-level fall, triggering headward erosion, stream piracy effects, and drainage inversion. The mapped river inversions and catchment piracy were related with the distribution of a quantile regression of 134 alluvial fans Vs basin areas. Despite the two parameters are well-fitted by a power law relationship, all the fans corresponding to captured rivers lay above the regression line (in the fan area field), whereas those corresponding to capturing rivers, are below the regression line (in the basin area field).

We propose a general model of alluvial-fan growth in active extensional settings that helps interpret the scatter of fan vs basin areas distribution and to identify the most active fault segments. Such approach can better constrain fault activity in a time-window which bridges long-term deformation to present-day deformation inferred from geodesy and/or seismology increasing our understanding of fault steadiness/unsteadiness behaviour.

**keywords:** continental extension, alluvial fans, drainage response to faulting; sedimentary record of fault-bounded basins, stream piracy, Northern Apennines

Integration of different approaches, each best suited for different temporal scales, from tens of thousands to millions of years, helps unravel the spatial and temporal evolution of active tectonic environments. The combination of datasets at different time-scales with present-day geodetic and seismological data can help understand the seismogenic potential of master faults as well as and the activity of single fault segments (Keller, 1986; Leeder and Gawthorpe, 1987; Stewart and Hancock, 1994; Frankel and Pazzaglia, 2006; Burbank and Anderson, 2012).

At long time-scales ( $10^5$  to  $10^6$  yr), the analysis of sediment records in fault-controlled extensional basins provides valuable information on the space-time evolution of active tectonics (Gawthorpe and Leeder, 2000) and on the mid- to long-term growth of individual fault segments (Jackson and Leeder, 1994).

A number of issues hampers the investigation of the sedimentary records in fault bounded basins. In settings characterized by a regional uplift, for example, the efficiency of normal faults in promoting hanging-wall subsidence is counterbalanced by erosion induced by regional uplift, which can reduce the volume of sediments delivered into the basins (Doglioni et al. 1998; Pucci et al. 2014). In addition, if active extension migrates, a shift occurs also in the position of the active depocenter (Gawthorpe and Leeder, 2000).

At short geological time-scales (up to  $10^5$  yr), the spatial variation of active tectonics can

50 produce peculiar geomorphological features characterized by wind gaps, abandoned valleys,  
51 stream captures and drainage inversions (Pazzaglia, 2003; Molin et al. 2004; Cowie et al.  
52 2006; Schiattarella et al. 2006; Picotti and Pazzaglia, 2008; Wegmann and Pazzaglia, 2009;  
53 Burbank and Anderson, 2012; Gioia et al., 2014).

54 A number of studies have shown that the geomorphological evidence of the landscape  
55 response to active extension (e.g., river anomalies) can be used to identify the (recent)  
56 evolution of normal faults, and to measure fault slip-rates and their temporal variations  
57 ( Goldsworthy and Jackson, 2000; Peters and Van Balen, 2007; Whittaker et al. 2008;  
58 Boulton and Whittaker, 2009; Di Naccio et al. 2013).

59

60 Alluvial fans, a common geomorphological feature in different climatic regions and tectonic  
61 environments, are known to be key indicators of active tectonics, chiefly in the Quaternary  
62 (Bull, 1977, 1991, Ritter et al. 1995; Harvey, 2002).

63 In many regions Pleistocene alluvial fans are not only indicators of tectonic activity, but are  
64 also related to an increase in sediment transport soon after a main glacial period. In the  
65 Mediterranean area, during the Pleistocene cold stages, the upper catchments of  
66 mountainous regions were subjected to intense periglacial processes and sustained snow  
67 packs, even at relatively low elevations, with a resulting increase of sediment supply and  
68 formation of alluvial fans in the lowlands (Hughes and Woodward, 2017). Examples were  
69 described from Montenegro (Adamson et al., 2017), from Greece (Pope et al., 2017), as well  
70 as from the Apennines of Italy (Giraudi et al., 2011; Giraudi and Giaccio, 2017).

71

72 Active tectonics of basin margins controls the build-up of alluvial-fans and their variability,  
73 geometry and internal structure (Hooke, 1967; Blum and Törnqvist, 2000; Gibling et  
74 al.2011; Harvey et al. 2005). Tectonic forcing influences the morphology of the alluvial fans,  
75 providing the relief potential, increasing energy gradients along the river network that  
76 delivers sediments to the fan.(Ethridge and Wescott, 1984, Silva et al. 2003, Calvache et al.  
77 1997; Barrier et al. 2010).

78

79 Various studies have revealed a correlation between morphometric measures of alluvial fans  
80 and their contributing catchments, including e.g., the ratio between the area of the fan and  
81 the area of the contributing catchment (Harvey, 1987), and the ratio between the fan slope  
82 angle and the average terrain gradient in the catchment (Viseras et al. 2003). The correlation  
83 also depends on local/regional environmental and tectonic settings (Harvey, 1987; Ferrill et  
84 al. 1996; Guzzetti et al. 1997; Sorriso-Valvo et al. 1998; Harvey et al. 1999; Viseras et al.  
85 2003; Mather et al. 2015).

86

87 Here, we address the issue of how the investigation of the recent geological history of a  
88 fossil alluvial fan system can provide information on the time and space migration of active  
89 tectonics and the resulting reorganization of the river network. We study how the  
90 reorganization of the river network causes river piracy, increasing the contributing area of  
91 some catchments at the expense of nearby catchments, and how this affects the statistics of  
92 the area of the fans and the catchments.

93 For the study, we selected the Bastardo and Foligno valleys, in the Northern Apennines of  
94 Italy (Fig. 1), a Pliocene-Pleistocene continental basin characterized by braided rivers and  
95 shallow lakes (Ambrosetti et al. 1987; Conti and Girotti, 1977; Bucci et al. 2016a). The area  
96 is tectonically active, with extension rates in the range 2.5-2.7 mm/yr (Hunstad et al. 2003;  
97 D'Agostino et al. 2009), and instrumental and historical seismicity (maximum epicentre  
98 intensity  $I_0 = VIII$ , Rovida et al., 2011).

99

100

101

## 102 **Geological setting**

103 The study area is characterized by a gentle hilly morphology shaped on the flanks of the  
104 Montefalco ridge, about 400 m a.s.l. West of the ridge, in the Bastardo valley (Gregori,  
105 1988), elevation is about 300 m a.s.l., whereas in the eastern Foligno valley it is about 200 m  
106 a.s.l. To the W and to the E of the study area, the Umbria-Marche Apennines provide the  
107 highest reliefs (about 1,070 m the Martani range, and 1,250 m the Foligno Mountains). The  
108 present-day climate of the area is temperate sub-continental Mediterranean, warm and dry in  
109 the summer and mildly cold in winter. In the area, the Topino River represents the main  
110 drainage system, which originates in the Apennine chain and flows from NE to SW toward  
111 the Foligno Valley (Fig. 1a). A main tributary of the Topino River is the Teverone River, that  
112 flows towards the NNW within the Foligno Valley. This river, in turn, collects the waters of  
113 the Attone River, draining the E portion of the Bastardo valley (Fig. 1a).

114 The Montefalco ridge dominates the Foligno valley towards E and the Bastardo valley  
115 towards W (Fig. 1a). These two valleys are shaped on the continental sequence deposited  
116 within the ancient “Tiberino lake”, a depositional environment characterized by braided  
117 rivers and shallow lakes of Pliocene to Pleistocene age (Conti and Girotti, 1977; Ambrosetti  
118 et al. 1987; Bonini, 1997; Coltorti and Pieruccini, 1997; Martinetto et al. 2014).

119

## 120 *Stratigraphy*

121

122 The continental sequence consists of a series of laterally discontinuous deposits separated by  
123 palaeo-topographic ridges and thresholds overlying unconformably the pre-existing bedrock  
124 constituted by the Umbria-Marche meso-cenozoic carbonatic multilayer (UM, Fig. 2a,  
125 Cresta et al. 1989) and the Miocene siliciclastic Marnoso Arenacea fm (MA, Fig. 2a, Ricci  
126 Lucchi, 1986).

127 The outcropping continental deposits consist of three main groups: (i) a basal grey clay  
128 member represented by fine grained flood-plain, lacustrine lignitiferous clay of Late  
129 Pliocene age (Lotti, 1926; Ge.Mi.Na., 1962; Follieri, 1977; Coltorti and Pieruccini, 1997;  
130 ISPRA, in press), which crops out SE of the study area (Morgnano, Fig. 1a); (ii) a sandy  
131 clayish locally lignitiferous sequence with subordinated conglomerate Early Pleistocene in  
132 age (Ambrosetti et al. 1987); and (iii) a detritic assemblage mainly composed of layered  
133 conglomerate and sand. Based on the available subsurface data (Ge.Mi.Na., 1962; Barchi et  
134 al. 1991), the maximum thickness of the deposits is estimated to be larger than 600 m under  
135 the Foligno valley. The maximum thickness of the deposits decreases W of the Montefalco  
136 ridge, where it is estimated to be less than 400 m (Bucci et al. 2016a). Here we refer to the  
137 revised stratigraphy by ISPRA (in press) and Bucci et al. (2016a), in particular:

138

- 139 (1) the *Bevagna Unit* (BU, Fig. 2b, Early Pleistocene), a fine-grained floodplain and  
140 lacustrine Unit, that corresponds to unit (ii) described above.
- 141 (2) the *Montefalco Unit* (MU, Fig. 2b, Early-Middle Pleistocene), composed of gravels  
142 and conglomerates of both fluvial and fan delta environment, overlying the Bevagna  
143 Unit. It corresponds to unit (iii) described above.
- 144 (3) the *Colle del Marchese Unit* (CU, Fig. 2b, Early-Middle Pleistocene), fan-type  
145 conglomerates with poorly sorted and poorly rounded pebbles pertaining to a  
146 partially fluvial and partially subaerial fan deposition environment, coeval with the  
147 Montefalco unit.
- 148 (4) the *Pianacce Unit* (PU, Fig. 2b, Middle-Late Pleistocene), a deposit consisting of  
149 dark reddish and brownish clays and sandy clays with few pebbles which  
150 unconformably overlies the Bevagna Unit and is present only in the central, flat part  
151 of the basin. This unit represents the youngest lacustrine deposit in the basin. The  
152 south-western part of the deposit is characterized by different facies composed of red  
153 silty clay with Mesozoic-Cenozoic carbonate clasts named as Fabbri member (FM –



- 154 Fig. 2b) by Bucci et al. (2016a), and interpreted as a palaeo-fan.  
155 (5) Alluvial deposits (AD, Fig. 2, Late Pleistocene-Holocene), fine-grained floodplain  
156 sediments made of gray and yellowish clays and sandy clays.  
157 (6) Alluvial-fans (AF, Fig. 2a,b Late Pleistocene-Holocene), coarse-grained fan-shape  
158 debris deposits in a silt and subordinately clay matrix.

159  
160 The stratigraphical, depositional and tectonic features of the continental deposits are  
161 summarized in Table 1. The age constraints of the outcropping deposits are scarce. Most  
162 ages are assigned on the basis of stratigraphic correlations with nearby deposits in similar  
163 structural and depositional settings. In particular, the Bevagna unit was assigned to the Early  
164 Pleistocene (Calabrian) on the basis of paleofloristic and palinological analyses (Ambrosetti  
165 et al., 1987). A recent paleomagnetic study by Bizzarri et al., (2011) performed in a quarry  
166 near Bevagna (Fig.2a) suggests that the uppermost part of this unit might be about 0.78 Ma.  
167 The Montefalco unit overlies the Bevagna unit. For these reasons it is considered to be  
168 Early-Middle Pleistocene in age.

169 These pieces of information on the age of both the Bevagna and the Montefalco units also fit  
170 with other evidences at a larger scale. About 50 km NW of the study area, still along the  
171 same continental basin (between Perugia and Città di Castello, see Fig. 1b) the Fighille unit  
172 (similar to the Bevagna unit) was assigned to the Early Pleistocene, ~1.8 Ma, by mollusk  
173 assemblages and mammal faunas (late Villafranchian, Tasso F.U., Ciangherotti and Esu,  
174 2000; Argenti, 2004; Masini and Sala, 2007). On top of the Fighille unit, a facies of  
175 conglomerates and sands similar to the Montefalco unit was assigned to the Early-Middle  
176 Pleistocene on the basis of mammal records (Colle Curti F.U., and Early-Middle Galerian,  
177 post- Colle Curti F.U., 1.0-0.8 Ma; Petronio et al., 2002; Argenti, 2004; Masini and Sala,  
178 2007).

179 The Colle del Marchese unit represents a proximal deposit which was emplaced by the rivers  
180 draining the M.Martani reliefs to the Bastardo valley: since it is in the same stratigraphical  
181 position of the Montefalco unit, the same Early-Middle Pleistocene age was inferred.

182 While the Montefalco e Bevagna units are mapped in both the Foligno and the Bastardo  
183 valleys, and represent the sediments deposited within the ancient “Tiberino Lake” (ISPRA,  
184 in press), the Colle del Marchese and Pianacce units are present only in the Bastardo valley  
185 (Bucci et al. 2016a) suggesting a differentiation of the sedimentation respectively W and E  
186 of the Montefalco ridge, after the end of the Early Pleistocene.

187  
188 The Foligno and Bastardo valleys significantly differ in terms of present day river incision  
189 (Fig. 2a). The Foligno valley is about 7-km wide, it is flat and occupied by alluvial deposits.  
190 Here, there are no river terraces and the most prominent feature on the E side of the valley is  
191 represented by the Foligno alluvial fan, a 35-km<sup>2</sup> wide feature built by the Topino River  
192 flowing from NE to SW (Gregori and Cattuto, 1986; Cattuto et al. 2005). The Foligno valley  
193 has not been recently affected by incision, as testified by the absence of river terraces. Here,  
194 the Pleistocene continental deposits crop out only along the western side of the valley  
195 (Fig. 2a). On the contrary, the Bastardo valley is presently incised by the river system. The  
196 resulting morphology is gently hilly with remnants of erosional terraces (Bucci et al. 2016a).  
197 Incision is carved within the continental deposits which crop out within the basin, and only  
198 few alluvial deposits are concentrated along the valleys of the Puglia and the Attone Rivers.  
199 These two rivers form the divide between the waters flowing towards the Topino-Teverone  
200 streams to the E, and those flowing towards the Tiber River to the W (Fig. 2a).

## 201 202 *Tectonics*

203  
204 Both valleys are elongated in a NW-SE direction, and bordered by a set of NE-dipping and  
205 SW-dipping normal faults (Barchi et al. 1991). The recent activity of the basin-bounding

206 normal faults is testified by geological evidence, including e.g., faulted Pleistocene deposits  
207 (Barchi et al. 1991; Brozzetti and Lavecchia, 1995) and stream captures (Gregori and  
208 Cattuto, 1986; Gregori, 1988; Cencetti, 1990).  
209 The normal faults belong to a well-known set of NW-SE striking faults that represent the  
210 youngest extensional structures which dissect the previously formed Northern Apennines  
211 (Fig. 1b), an Oligo-Miocene, east-verging fold and thrust belt later affected by extension  
212 (Malinverno and Ryan, 1986; Martini and Sagri, 1993; Barchi, 2010).  
213 The W to E migration of compression-extension produced a characteristic setting, in which  
214 extension is always superimposed on compression (Lavecchia et al. 1994; Doglioni et al.  
215 1999; Pascucci et al. 2006; Pauselli et al. 2006; Barchi, 2010). Compression is presently  
216 active all along the Adriatic coast, whereas extension is active along the axial culmination of  
217 the Northern Apennines. Present day geodetic data indicate active SW-NE extension rates  
218 along a NW-SE alignment of 2.5-2.7 mm/yr (Hunstad et al. 2003; D'Agostino et al. 2009).  
219 The recent tectonic history of the area reflects in the historical seismicity, which shows that  
220 the area was struck by several earthquakes with  $M \geq 5$  (Rovida et al. 2011) (Fig. 1a).  
221 Instrumental seismicity shows constant earthquakes release, and the available focal solutions  
222 provide nodal planes striking mainly NW-SE (Pondrelli et al. 2006).  
223 At the regional scale, crustal extension is accommodated by a set of six sub-parallel E-  
224 verging low angle detachments, which have driven the onset of the hinterland extensional  
225 basins of the Northern Apennines (Barchi et al. 1998; Pauselli et al. 2006). In the area, the  
226 low angle detachment is represented by the Alto Tiberina Fault (ATF), an ENE-dipping low  
227 angle normal fault, the easternmost, youngest and presently active detachment (Barchi et al.  
228 1998; Collettini and Barchi, 2002; Chiaraluce et al. 2007), which has accommodated up to  
229 10 km of extension in the last 3 Myr (Mirabella et al. 2011; Caricchi et al. 2015). The  
230 superposition of extension on the already emerged compressional edifice brought a  
231 significant modification on the existing drainage pattern. At the end of the Late Cenozoic,  
232 when the fold-and-thrust belt emerged, rivers were draining mainly to the E, following the  
233 main regional slope and, in places, following the main arc-shaped valleys formed in  
234 correspondence of major synclines (Alvarez, 1999 and references therein). The onset of  
235 extension changed the relative elevation at the normal faults hanging-wall and footwall,  
236 forming a new landscape with new depocenters where the sediments could flow and deposit.  
237 The modification produced drainage inversions and stream captures in the area (Gregori and  
238 Cattuto, 1986; Cattuto and Gregori, 1988; Cattuto et al. 1988; Cencetti, 1988, 1993; Gregori,  
239 1988, 1990) and elsewhere in the Northern Apennines (e.g., D'Agostino et al. 2001;  
240 Bartolini et al. 2003; Fidolini et al. 2013).

241  
242

## 243 **Methods**

244

245 To understand the recent landscape modification caused by the active extension and the  
246 consequent river captures in the Bastardo and Foligno valleys, we combined field-based  
247 geological surveys, surface and sub-surface geology data, and detailed photo-geological  
248 mapping of the continental deposits. We performed field surveys to identify and measure the  
249 geometry and kinematics of the faults affecting the continental Quaternary sequence, and to  
250 measure palaeo-current data. Sub-surface geological data consisted of the interpretation of  
251 two high-resolution seismic reflection profiles in the Foligno valley, which portray the  
252 subsurface geometry of the latest basin infill close to the Montefalco ridge (traces Fo1 and  
253 Fo2 in Fig. 2a). The geomorphological analysis consisted in mapping the drainage pattern  
254 anomalies and stream captures, in comparing the present-day river network to palaeo-rivers  
255 deposits, and in the analysis of the present-day area of the alluvial fan and their contributing  
256 catchments. Furthermore, we analysed the long-profiles slope of the most representative  
257 streams crossing the recent-most normal faults on the NE-flank of the Montefalco.

258

259 *Surface geology*

260

261 We performed field-work to characterize the sedimentology of the continental deposits and  
262 the geometry and kinematics of the faults affecting the deposits. We integrated the  
263 sedimentological and structural information with a recent photo-geological map at 1:25,000  
264 scale (Bucci et al. 2016a), and we compared this information with the existing geological  
265 and geomorphological maps, at different scales (Servizio Geologico d'Italia, 1969; Gregori,  
266 1988; Cencetti, 1990, 1993; Regione Umbria, 2015a). The sedimentological data include the  
267 attitude of imbricate clasts within the conglomerates, that provides information on the  
268 provenance of the palaeo rivers. We computed the clustering of the orientation data using the  
269 1% area contouring method and the mean value for the dip direction and plunge of the  
270 imbricate clast using Fisher statistics (Fisher et al. 1987). In addition, we treated dip  
271 directions of imbricate clasts as directional data, and compared our original data with  
272 published palaeo-current direction indicators. To analyse the structural data, including the  
273 attitude of fault planes and the orientation of fault slip indicators, we adopted the procedure  
274 proposed by Marrett and Allmendinger (1990), and Allmendinger et al. (2012). To quantify  
275 the relationships between the orientation of the fault populations and the slip vectors, we  
276 calculated the b-axis along fault systems, adopting the procedure proposed by Roberts  
277 (2007).

278

279 *Subsurface data*

280

281 We used high resolution seismic reflection data which provide information on the internal  
282 geometry of both the continental units and the tectonic structures at depth, and give  
283 constrains on the recent-most tectonic activity of the basins-bounding fault E of the  
284 Montefalco ridge. The E part of the Foligno valley is crossed by two high resolution seismic  
285 reflection profiles (Fo1 and Fo2, Fig. 2a) which were acquired by the Regione Umbria  
286 (2015a) in the framework of a regional geological cartography project. The two lines are  
287 1.15 and 1.40 km long, respectively, and provide a good quality image up to about  
288 0.8 second TWT (two-way-time traveling velocities of the seismic rays). According to  
289 published data, the interval velocity of the continental deposits is ~2.0 km/s (Bally et al.  
290 1986; Buonasorte et al. 1988), which means that the profiles provide a detailed image of the  
291 upper part of the continental sequence, including the alluvial deposits i.e., up to a depth of  
292 about 800 m.

293

294

295 *Geomorphological analysis*

296

297 We executed a detailed, multi-scale geomorphological analysis using a large dataset of  
298 stereoscopic aerial photographs taken at different times and scales. Specifically, we used (i) a  
299 black and white flight taken in 1954 at 1:33,000 scales, (ii) a black and white flight taken in  
300 1997 at 1:27,000 scale, and (iii) a colour flight taken in 1977 at 1:13,000 scale. The  
301 photogeological approach allowed us to map both geomorphological elements and  
302 geological and tectonic features including bedding indicators (e.g., lithological limits,  
303 Marchesini et al. 2013; Santangelo et al. 2015), structural features (e.g., faults and folds,  
304 Bucci et al. 2013, 2016b), sedimentary deposits (e.g., alluvial fans, alluvial deposits, Bucci  
305 et al. 2016a), and erosional features (e.g., erosional terraces, Bucci et al. 2016a). The  
306 geomorphological analysis focussed on a detailed inventory of the present-day alluvial fans,  
307 which we mapped together with their catchment areas. We analysed the river network to  
308 compare the present-day river paths to the distribution of the clastic deposits associated to  
309 palaeo-drainages, including the Montefalco conglomerates and the two fans pertaining to the

310 Colle del Marchese conglomerates (Fig. 2a). We mapped evidence of river captures and  
311 piracy effects in the area, we compared them to the present-day river network, and we  
312 integrated our dataset with pre-existing evidences of river piracy (Gregori, 1988; Cencetti,  
313 1990, 1993). In addition, as river long-profiles are known to register recent-most fault  
314 activity in different tectonic settings (e.g. Whittaker et al., 2007; Yanites et al., 2010 and  
315 therein references), we extracted the profiles of three rivers draining the NE flank of the  
316 Montefalco hill towards the Foligno valley to verify the possible correspondence between  
317 river anomalies (e.g. knick-points) and the mapped faults. The stream profiles were extracted  
318 from a 1:5.000 scale topographic map of area. To emphasise the knick-points which are due  
319 to local downstream changes in slope (dH) along the profile (dL) we plotted the downstream  
320 change in slope (dH/dL%) along the stream long-profiles.

321

## 322 **Results**

323

### 324 *Surface geology*

325

326 Our sedimentological data, integrated with data collected by Regione Umbria (2015a), show  
327 palaeo-currents clustered from the NE (Fig. 3a). The layers containing the imbricate clasts  
328 are sub-planar, or gently dipping to the SW (Fig. 3b). Palaeo-currents and bedding data  
329 indicate that the source area of the Montefalco conglomerate was located NE from the fan.  
330 The NE provenance of the sediments is further supported by a fining trend of the  
331 conglomerate from NE to SW, which indicates that the fan proximity is to the NE, close to  
332 the apex of the Foligno fan (Fig. 3 c, d).

333 The structural data concern faults that offset pre-Quaternary rock assemblages and  
334 Quaternary deposits (Fig. 4). Where evident, fault kinematics is mostly dip-slip, with a SW-  
335 NE trending direction of extension (Fig. 4 a, b), consistent with the Apennines regional  
336 strain field (Boncio and Lavecchia, 2000). Figure 4c shows the pole to the fault population  
337 obtained with the b-axis method for the Giano dell'Umbria fault system. The pole of the  
338 fault population is parallel to the striae measured in the pre-Quaternary carbonate rocks  
339 (Fig. 4d), and to the slip vector obtained for the striated fault of the Montefalco fault system  
340 (Fig. 4a). The findings reveal a dip-slip kinematics, with a top-to-the-NE direction for both  
341 the Montefalco and the Giano dell'Umbria fault systems.

342 Despite the kinematic similarities, the two fault systems show different relationships with the  
343 recent deposits. The map pattern (Fig. 2a) shows diffuse faulting of the pre-Quaternary rocks  
344 along the Giano dell'Umbria Fault system. Most of the faults cut the continental sequence,  
345 Early Pleistocene in age, but do not affect the sediments of the Pianacce Unit, Late  
346 Pleistocene in age, which are undeformed. No aggradation was found at the hanging wall of  
347 the Giano dell'Umbria Fault system, where fluvial incision exposes the basal unconformity  
348 between the pre-Quaternary rocks assemblages and the Quaternary continental deposits.  
349 These evidences constrain the activity of the Giano dell'Umbria Fault system up to the  
350 Early-Middle Pleistocene. In contrast, the Montefalco Fault system is characterized by a  
351 staircase geometry (Bucci et al. 2016a) developed within the sediments of the Bevagna and  
352 the Montefalco units, Early-Middle Pleistocene in age. The map pattern reveals that the  
353 lower fault strand bounds the present-day aggrading plain of the Foligno basin, suggesting  
354 the involvement of Holocene deposits in the active faulting along the base of the Montefalco  
355 ridge.

356 Overall, the structural analysis indicates the geometry and the kinematics of the studied fault  
357 systems, consistent with those of other Quaternary faults in the Northern Apennines  
358 (Brozzetti and Lavecchia, 1995; Boncio and Lavecchia, 2000). Evidence of recent (Late  
359 Quaternary) faulting is recognized along the Montefalco Fault system, whereas evidence of  
360 fault activity is constrained to the Early-Middle Pleistocene along the Giano dell'Umbria  
361 Fault system.

362

363

364 *Seismic reflection data*

365

366 The line Fo1 is characterized by a clear lateral heterogeneity (Fig. 5a). The seismic signal  
367 sharp change is confirmed by the velocity analysis that indicates, in the SW part of the line  
368 Fo1, at the CMP 30, a mean velocity in the range between 1900 m/s and 2100 m/s, up to  
369 about 150 m/s TWT, whereas for the CMP 205 the same velocity is observed up to about  
370 470 m/s TWT. Line Fo1 shows a set of chaotic, NE-dipping reflectors which correspond at  
371 surface with the trace of the NE-dipping normal faults, bordering the Foligno valley  
372 (Fig. 5a). These reflections, which we interpret as the subsurface expression of the normal  
373 faults, are in contact with a set of sub-horizontal reflectors at the fault hanging-wall, which  
374 identify the presence of a stratified sedimentary sequence interpreted to be the Bevagna  
375 Unit .

376 The line Fo2 does not show a significant lateral velocity variation up to 800 m/s TWT. The  
377 mean velocity of this line is the same observed in Fo1 for CMPs greater than 205, and TWT  
378 greater than 470 ms. The obtained mean velocities are in agreement with the published data  
379 for the continental deposits i.e., about 2000 m/s (Bally et al. 1986; Buonasorte et al. 1988).  
380 The Fo2 seismic profile (Fig. 5b) shows that the Bevagna Unit prosecutes down to at least  
381 0.8 sec (TWT), corresponding to about 800 m, a depth similar to other continental basins  
382 along the upper Tiber River valley NW of the study area (Barchi and Ciaccio, 2009; Pucci et  
383 al. 2014). The Bevagna Unit is characterized by a significant tilt of the beds towards SW  
384 (Fig. 5b). The amount of tilt decreases towards the surface and we interpret this as the  
385 evidence of syn-depositional, NE-dipping fault activity. The depth conversion of the seismic  
386 data indicates a tilt in the order of 3° to the SW (Fig. 5c). The upper part of the Fo2 seismic  
387 line shows a more chaotic pattern, which we interpret as due to the presence of a thick  
388 alluvial sequence (Fig. 5 a,b). The interpretation is further supported by deep water wells in  
389 the area, which provide a maximum thickness of the alluvial deposits of about 150 m  
390 (Regione Umbria, 2015b).

391

392

393

394 *Geomorphology*

395

396 **River captures.** We mapped the evidences of river captures and drainage inversion as  
397 derived by the rivers network and the morphology of the area (Fig. 6). In the E part of the  
398 study area we mapped several captures of rivers pertaining to the Menotre River network  
399 (Fig. 1, 6), in agreement with the geomorphological map of Cencetti (1993). In particular,  
400 we find that the upper reach of the Menotre River (river n. 3 in Fig. 6) is part of a palaeo-  
401 river (i.e., the palaeo-Menotre) which was flowing in the opposite direction, to the South. We  
402 identify four possible watersheds of the palaeo-river which we interpret as the progressive  
403 reduction of the size of the palaeo-Menotre catchment before being definitively captured and  
404 inverted by the Topino River (Fig. 6). As a result, while the palaeo-Menotre drastically  
405 reduced its catchment, the Topino River increased its contributing area. The present-day  
406 Pettino stream (n. 6 in Fig. 6 and Fig. 1a) and Spina River (stream n. 7 in Fig. 6 and Fig. 1a)  
407 are remnants of the palaeo-Menotre River draining into the area of Campello sul Clitunno  
408 (Fig. 1, 6).

409 In the W part of the study area, we identified evidence of stream captures in the eastern flank  
410 of the Mt. Martani range towards the Bastardo Valley basin and along the Puglia and Attone  
411 River systems (Bucci et al. 2016a). Comparing the Colle del Marchese Unit outcrop with the  
412 position of the present-day river network, we find that there is no one-to-one correspondence  
413 between the location of the present-day rivers and the Pleistocene deposits (Fig. 2). The

414 north-western apron is re-incised but still connected to the drainage system of the Torinetto  
415 stream, a tributary of the Puglia river to the W (Fig. 2). On the contrary, the SE apron is  
416 disconnected from its original drainage system, suggesting that the main stream responsible  
417 for the conglomerates deposition was captured elsewhere, presumably in the present day  
418 Foligno valley which represents the active subsiding basin (Fig. 2). In this case, the captured  
419 river could be the Rovicciano stream (Fig. 2, and stream n. 15 in Fig. 6), a tributary of the  
420 Teverone-Topino rivers system to the east (Fig. 6). In the W part of the study area, the Attone  
421 and the Puglia Rivers form the watershed between the waters flowing to the NE and those  
422 flowing to the west (Fig. 2, 6). The peculiarity of the divide is that it lays in the Bastardo  
423 valley rather than along the alignment of the maximum elevations (Fig. 1a, 2). We interpret  
424 this finding as evidence that the Attone River has caused a strong headward erosion in  
425 response to the downthrow of the Foligno Valley since the Middle-Late Pleistocene. When  
426 headward erosion cut the topographic threshold represented by the bedrock E of Gualdo  
427 Cattaneo, the Attone River entered the pre-existing Bastardo valley, and expanded its source  
428 area capturing some of the rivers which were previously feeding the Puglia River. As a  
429 result, the Pianacce Unit, which represents the latest palustrine deposit, was incised. Deep  
430 incised gorges and hanging palaeo-valleys detected in the middle part of the Attone basin  
431 (Fig. 6) support this interpretation.

432

433 **Allometry of alluvial fans.** We mapped a total of 134 alluvial-fans and their catchments  
434 (Fig. 2). The fan planimetric area spans 4.5 orders of magnitude, from  $\sim 0.01 \text{ km}^2$  to  $\sim$   
435  $35 \text{ km}^2$  which is the size of the Foligno fan, built by the Topino River, (Fig. 2). The basin  
436 areas span about 5 orders of magnitude, from less than  $0.05 \text{ km}^2$  to about  $390 \text{ km}^2$  (the  
437 Foligno River basin). On a log-log plot, the cloud of the empirical points of fans areas ( $A_f$ )  
438 and basin areas ( $A_b$ ) shows a clear trend (Fig. 7a). Based on our data, we obtained a  
439 regression line fitting the data with equation,

440

$$441 A_f = 0.16A_b^{0.9}$$

442

443 Figure 7b shows a map of the alluvial fans and their contributing catchments which are  
444 related to rivers which were captured, or underwent capturing by a nearby river system as  
445 described in Fig. 6. In particular, we mapped as red the fans and catchments which are  
446 related to captured rivers and dark grey/black the fans related to capturing rivers. With the  
447 same colours, we show the position and number of the fans in Fig. 7a. The data comparison  
448 shows that the fans of capturing rivers (dark grey/black) are systematically placed below the  
449 regression line, whereas the fans of captured rivers are above the regression line (Fig. 7a).  
450 Below we report some specific examples of rivers drainage inversions and captures.

451 The identified stream piracies, combined with the alluvial-fan areas and their catchments  
452 areas, allowed us to identify some rivers which included nearby catchments into their  
453 contributing areas. The present-day Topino River (n. 3 in Fig. 7) captured the palaeo-  
454 Menotre River leaving two rivers, Pettino (n. 6) and Spina (n. 7) the fans of which are too  
455 large for their current catchments (Fig. 7). The capture operated by the Topino River also  
456 affected fans n. 4 and 5, which are also too large for the size of their catchments (Fig. 7a).  
457 The Topino River basin (n. 2 in Fig. 7) also captured the Menotre River, the fan of which is  
458 very small compared with the catchment size (n. 3 in Fig. 7). We interpret these features as  
459 evidence of the progressive capturing operated by the Topino River, reflected in the presence  
460 of the intra-catchment fans which plot above the regression line. As a result of the repeated  
461 captures, the shape of the Topino catchment is elongated in a direction that is orthogonal to  
462 the Foligno fan feeding channel, and extends northward and southward (Fig. 7b), sub-  
463 parallel to the active fault bounding eastward the Foligno valley.

464 On the other side of the Foligno valley, the fan areas are smaller mainly because of the low  
465 relief of the catchments (Fig. 6, 7). Here, the largest catchments are those corresponding to

466 fans n. 14 and n. 15, which are far smaller compared to their contributing areas. Such  
467 catchments are the result of stream piracy. In particular, stream n. 15 (Figs. 6, 7) captured the  
468 Rovicciano stream, which was draining the SE apron of the Colle del Marchese Unit. To the  
469 N of Montefalco, fan n. 17 captured the drainage area of fan n. 16.  
470 A peculiar case is represented by the Attone River (n. 18, Fig. 2, 6, 7), with a basin that  
471 extends for 60 km<sup>2</sup>, and no morphological evidence of an alluvial fan (see star on the basin  
472 area axis in Fig. 7b). According to the size of the basin, the expected fan should be of ~  
473 6 km<sup>2</sup>. We hypothesize that the absence of such a large fan is due to the fact that when the  
474 Attone River entered the Bastardo valley, due to progressive headward erosion, it found an  
475 area already characterized by a gentle topography, with a low local relief that prevented  
476 erosion and transport. The hypothesis is supported by the evidence that the Attone River is  
477 depositing sediments in the Bastardo valley, far from its outlet in the Foligno valley (Fig. 2).  
478 However, we cannot exclude that a fan deposit rests below the topographic surface at the  
479 outlet of the Attone River, covered by the recent-most alluvial deposits. This indicates high  
480 aggradation rates, in agreement with active tectonic subsidence expected at the hanging-wall  
481 of the Montefalco Fault. Geo-archaeological evidence, consisting of remnants of a Roman  
482 Temple of 1700 years ago, sealed by 2 m thick alluvial deposit (Colacicchi and Bizzarri,  
483 2008), seems to confirm an aggradation rate in the order of 1.17 mm/year at the outlet of the  
484 Attone River.

485  
486 **River long-profiles.** We extracted three stream long-profiles from the Mauro, La Fornace  
487 and La Torre streams, which we consider representative of the rivers draining the NE-flank  
488 of the Montefalco hill from SW to NE (Fig. 8a). The streams range in length between 1000  
489 and 2500 m, and they flow on the Montefalco unit mostly composed of conglomerates with  
490 abundant sand and clay layers. Visual inspection of the stream profiles reveals clear knick-  
491 points, the most prominent of which are well evidenced by the slope variation (dH/dL%, Fig.  
492 8a), in good agreement with the mapped NE-dipping normal faults (Fig. 8b). We note that  
493 some of the knick-points are due to the presence of deep-seated landslides, which are  
494 abundant in the area (Bucci et al., 2016a), and to less erodible layers.  
495 The correspondence between the faults and the knick-points evidences that the faults were  
496 active very recently. In addition we point out that the lowest knick-point along the stream  
497 profile (red star in Figure 8b, c) clearly affects the present-day alluvial-fan suggesting that  
498 the fault is active also during the Holocene.

499  
500  
501  
502

### 503 **Morphotectonic evolution**

504

505 We recognize three main stages of the Quaternary morphotectonic evolution of the area  
506 (Fig. 9).

507 First, the initial formation of the ancient “Tiberino Lake” during the Early Pleistocene was  
508 due to the activity of the normal faults bounding the basin. Subsidence produced the  
509 accommodation space for the deposition of the Bevagna Unit and of the Montefalco gravels  
510 up to the Middle Pleistocene (Fig. 9a). In the W part of the study area, the Colle del  
511 Marchese Unit was deposited by rivers flowing from the Martani range into the basin,  
512 including the palaeo-Torinetto and the palaeo-Rovicciano streams. During this stage, the  
513 Puglia River was flowing to the SE into the present day Bastardo valley, and the Menotre  
514 River was still flowing to the SW into the present day Foligno valley. The main divide  
515 followed the alignment of the highest ridges (Fig. 6).

516 Second, the activity of the NE-dipping fault which (presently) borders the Montefalco hill to  
517 NE increased, hence downthrowing the Foligno valley and uplifting the Montefalco alluvial

518 fan at its footwall (Fig. 9b). The event resulted in the establishment of two distinct  
519 sedimentary basins, the Foligno and the Bastardo valley, respectively E and W of the newly  
520 formed Montefalco ridge. The Bastardo valley hosted an endorheic basin, where a palustrine  
521 environment developed, testified by the deposition of the Pianacce Unit (Fig. 2, 9b). The  
522 deactivation of the Montefalco fan produced a (complete) re-organization of the drainage  
523 network, inducing a change in the position of the alluvial fans position and the size of the  
524 contributing catchments. On the other hand the lowering of the Foligno valley triggered  
525 headward erosion of the Attone, Topino, and Menotre Rivers. This stage is also marked by a  
526 stream capture of the palaeo Rovicciano stream which was diverted from its original NE  
527 direction towards the Spoleto valley to the SE. This is testified by the fact that the (two)  
528 Colle del Marchese gravels deposits which were formed by two NE flowing rivers have a  
529 different relationship with the present-day river network. Whereas the NW deposit is still  
530 connected to a river i.e., the Torinetto stream, the palaeo-Rovicciano stream is no longer  
531 connected to a river and the Rovicciano stream was captured towards the SE (Fig. 6, 9c).  
532 Third, the last stage consisted in the further downthrowing of the Foligno valley, which  
533 produced enhanced stream headward erosion (Fig. 9c). The erosional event induced the  
534 Puglia and the Attone Rivers to enter the Bastardo valley, and triggered the onset of incision  
535 of the Pianacce Unit (Fig. 9c). As a result, the present-day divide is located in the centre of  
536 the Bastardo valley. We suggest that this differentiation occurred likely between the Late  
537 Pleistocene and the Holocene. In order to provide better constraints on the age of the two last  
538 evolution stages, it would be needed to have data about the timing of the river captures as  
539 testified by the age of the Pianacce Unit within the Bastardo valley. Unfortunately, to date,  
540 no good fauna content within the unit has been found which can provide an absolute age,  
541 and the only information is from relative dating obtained by stratigraphic relationships.  
542 Headward erosion of the Topino River reached the catchments of the palaeo-Menotre River  
543 inverting the course of the Menotre River. As a result, the present-day shape and size of the  
544 Topino catchment is wide, and elongated orthogonally to the outlet direction (Fig. 6, 9c).

545

546

547

## 548 **Discussion**

549

### 550 *A fossil alluvial fan*

551

552 The Montefalco alluvial fan is fossil, and down cut on the NE flank by a set of normal faults  
553 responsible for the deepening of the Foligno valley. The fan is presently about 100 m higher  
554 in elevation than the Bastardo valley to the W, and about 200 m higher than the Foligno  
555 valley to the E. The Montefalco fan delivered materials into a gulf of the ancient “Tiberino  
556 Lake”, represented by the Bastardo valley. Today, the valley is incised by the Puglia and the  
557 Attone rivers, whereas active subsidence characterizes the Foligno valley occupied entirely  
558 by alluvial deposits. The Montefalco conglomerate overlies the Bevagna Unit. Stratigraphic  
559 correlations, faunistic assemblages that correlate with the Tasso faunal units (Rook et al.,  
560 2010), and palaeomagnetic measurements (Gliozzi et al. 1997; Bizzarri et al. 2001), concur  
561 in establishing an age for the Bevagna Unit between ~ 1.8 and 0.78 Myr. We conclude that  
562 the drainage inversion caused by the uplift of the Montefalco fan is younger than 0.78 Myr.  
563 If we consider the 200 m difference in elevation between the top of the Montefalco hill and  
564 the Foligno valley as a proxy for the vertical component associated to the extension in the  
565 last 0.78 Myr, we infer a minimum vertical deformation rate of ~ 0.25 mm/yr, similar the  
566 slip-rates along the same alignment of normal faults in the upper Tiber River valley, NW of  
567 the study area (Fig. 1b, Pucci et al. 2014).

568 The high resolution seismic reflection profiles in the Foligno valley show that the alluvial  
569 deposits in the valley reach at least 150 m of thickness . The seismic reflection line (Fo1)



570 shows that the continental infill below the alluvial deposits is at least 700-800 m thick. The  
571 reflectors underneath the fluvial deposits are tilted towards SE, testifying the activity of the  
572 NE-dipping fault bordering the Montefalco ridge in the Holocene.  
573 Previous work (Gregori, 1988) depicted a tectonic evolution in which a master fault dipping  
574 to the SW first created the Foligno valley. This was followed by the activation of a NE-  
575 dipping fault bordering the valley, and by the migration of the active subsidence from E  
576 (Foligno valley) to W (Bastardo valley). The main implication of this interpretation was that  
577 the Montefalco conglomerate flew from the SW (Gregori and Cattuto, 1986; Cattuto et al.  
578 2005). We discard this interpretation because, based on our data, we infer that the  
579 Montefalco fan represents an ancient analogue of the present-day Foligno fan (Fig. 3d) built  
580 by the Topino River flowing from NE to SW. Our interpretation is supported by the presence  
581 of small outcrops of the Montefalco Unit near the town of Foligno (locality “I Cappuccini”,  
582 Fig. 2). These deposits, laying at about 315 m of elevation, exhibit the same lithology and  
583 the same depositional environment as the Montefalco deposits. Moreover, the size of the  
584 clasts is larger than those on the Montefalco hill (Fig. 3b), and their roundness is lower than  
585 the gravel found in the Montefalco hill, indicating a more proximal depositional  
586 environment. We interpret the deposit of the Montefalco Unit in the Foligno area as a  
587 remnant of the palaeo-fan which was built by a palaeo-Topino River before the activation of  
588 the Montefalco Fault system. The activation of this fault system induced subsidence in the  
589 Foligno valley and the deactivation of the Montefalco fan which was uplifted at the normal  
590 fault footwall.

591

#### 592 *Late Pleistocene - Holocene normal faults activity*

593

594 Extensional tectonics reached the study area in the Late Pliocene - Early Pleistocene (Barchi,  
595 2010). Today, the extension rates are  $\sim 2.7$  mm/yr (Hunstand et al. 2003; D’Agostino et al.  
596 2009) and interact with a regional uplift of  $\sim 0.5$  mm/yr, which has affected the area since  
597 about 1.5 Myr (Ambrosetti et al. 1982a, 1982b; Cinque et al. 1993; D’Agostino et al. 2001).  
598 The interaction produced a configuration in which the active subsiding basins do not always  
599 coincide with the active depocenters, depending on the balance between the efficiency of the  
600 basin-bounding faults in producing subsidence and the regional uplift. Where normal faults  
601 are efficient in producing subsidence at rates larger than the regional uplift, mainly  
602 aggradation occurs. Conversely, where normal faults are active but their vertical component  
603 rate is lower than the regional uplift, incision prevails (Pucci et al. 2014).

604 Today, the Foligno valley is flat and infilled with a thick sequence of alluvial deposits (about  
605 150 m). We interpret this configuration as evidence of the valley being subsiding, despite the  
606 regional uplift of the Apennines.

607 Previous studies showed that a 600 m – thick Pleistocene sequence is present underneath the  
608 alluvial deposits (Barchi et al. 1991). The upper-most part of this sequence is shown by the  
609 high-resolution profile Fo1 (Fig. 5) down to about 800 m. Considering the presence of the  
610 Pleistocene sequence and of the overlying thick alluvial deposits, as well as the absence of  
611 river terraces, we conclude that the Foligno valley has been a subsiding basin roughly  
612 continuously since the Early Pleistocene.

613 Along the same fault system, NW of the study area there exist three extensional basins  
614 elongated in a SE-NW direction (Ponte Pattoli, Umbertide, and Sansepolcro, Fig. 1b).

615 Previous studies suggested that the three basins behave differently in terms of the basin  
616 bounding faults efficiency in producing active subsidence (Melelli et al. 2014; Pucci et al.  
617 2014). In particular, it was suggested that the Ponte Pattoli and Umbertide basins are  
618 subsiding at rates smaller than the Sansepolcro basin, which is similar to the Foligno valley.

619 Also in the Sansepolcro valley, similar values of Pleistocene continental sequence (about  
620 1.2 km, Barchi and Ciaccio, 2009) and of alluvial deposits (about 150 m) are found together  
621 with the absence of river terraces (Pucci et al. 2014). The Foligno and the Sansepolcro basins

622 differ from the Ponte Pattoli and Umbertide basins also in terms of historical seismicity. In  
623 the Foligno and Sansepolcro basins the historical seismicity shows a maximum epicentral  
624 intensity  $I_0 = VIII$  (Rovida et al., 2011), whereas in the area between Ponte Pattoli and  
625 Umbertide only a few events of smaller intensity have been recorded. In our interpretation,  
626 the difference in the active subsidence revealed by the greater thickness of the alluvial  
627 deposits and the absence of river terraces, coupled with the more intense historical  
628 seismicity, suggest that differences exist in the basin bounding normal fault rates in creating  
629 hanging-wall subsidence.

630

### 631 *Role of pre-existing topography*

632

633 The superposition of different tectonic environments results in significant differences in the  
634 evolution of topography, and the corresponding pattern of the drainage network (Mazzanti  
635 and Trevisan, 1978). In our study area, the Miocene collisional tectonic phase produced a  
636 topography characterized by mountains separated by valleys that coincided with the axial  
637 culminations of anticlines and synclines, which controlled the position of the main divides  
638 and rivers. The reconstruction of the palaeo-Menotre River flowing to the S is an example of  
639 a river which flew according to the geometry of the contractional ridges, following a valley  
640 formed in a thrust-related syncline (Fig. 9) Along with these major topographic features,  
641 several transverse drainages developed as a result of simple antecedence (Burbank et al.  
642 1996) or a combination of antecedence and superposition (Mazzanti and Trevisan, 1978;  
643 Alvarez, 1999).

644 The pre-existing drainage pattern was inherited by the younger drainage network that  
645 developed starting from the onset of Quaternary extension. The effect of the extensional  
646 tectonics was to produce or to enhance new depocenters where the rivers discharged their  
647 sediments, and to form new high areas at the footwall of the normal faults, causing river  
648 headward erosion. Where headward erosion reached a previously low topographic area (e.g.,  
649 a pre-existing valley), the drainage area increased suddenly through the capture of pre-  
650 existing catchments. This is the case of the Attone River (Fig. 2, and river n° 18 in Fig. 6).  
651 As a result, some catchment is anomalously large with respect to the size (area) of its alluvial  
652 fan. Differences in river erosion and catchment areas can also be due to the different  
653 erodibility of the rocks in the catchments. However, in the study area we observe similar  
654 anomalies in terms of erosion and alluvial fans catchment areas for rivers draining different  
655 lithology domains like carbonate rocks, siliciclastic deposits and continental units. On these  
656 bases, we suggest that some of the data scatter in a fan area – contributing area plots are due  
657 to tectonic effects, which in turn induced river piracy.

658 We observe the same pattern in many alluvial fans. Matching geomorphological  
659 observations with the plot of the fan area – catchment area, we find that with respect to the  
660 average, the fans that were captured lay above the regression line, and the catchments that  
661 captured other streams lay below the regression line (Fig. 7a). As an example, the fans n. 4,  
662 5, 6 are 7 are too large for their current contributing area and are expected to deliver less  
663 sediments than they did in the past. Part of their contributing areas were captured by the  
664 Topino (n. 2) and of the Menotre (n. 3) rivers, which, on the contrary, are expected to deliver  
665 more sediments than they did before capture.

666

### 667 *A model for alluvial-fan growth in an active extensional setting*

668

669 In continental environments, the development of alluvial-fan successions, their shape and  
670 size, and the variability of their architecture are controlled by the tectonics of the basin  
671 margins, and the climate influence on denudation and discharge of water and sediments  
672 (Blum and Törnqvist, 2000; Gibling et al. 2011). The distribution of the fan areas versus  
673 their catchments is linear in log-log plots, and most Authors relate the data scatter to the

674 different tectonic environment (extensional, compressional) and sediment discharge related  
675 to climate (latitude and relief) (Guzzetti et al. 1997; Mather et al. 2000; Viseras et al. 2003;  
676 Harvey, 2002, Harvey et al., 2005).

677

678 We point out that the regression fittings average empirical data which can mask very  
679 different conditions. Our results suggest that part of the data-scatter may be related to the  
680 dynamic evolution of the fans, affected by catchment piracy operated by rivers at the  
681 expenses of nearby rivers. As shown in Fig. 7, we find that fans of capturing rivers are  
682 systematically below the regression line, whereas fans of captured rivers are above the  
683 regression line, as a result of river captures. Basing on geomorphological analysis (Fig. 6),  
684 we are able to distinguish data which are clearly related to stream piracy effects with a  
685 consequent significant difference in the meaning of the fan and catchment areas.

686

687 Based on our data and observations, we propose a model of alluvial-fan growth in active  
688 extensional settings as described in Fig. 10. Let us consider a continental extensional basin  
689 where a series of alluvial-fans draining the footwall of basin-bounding normal faults. The  
690 increase in activity of one fault of the fault system increases the subsidence of the hanging-  
691 wall block, and promotes headward erosion at the fault footwall, with a consequent  
692 enlargement of the catchment size (Fig. 10, stage a). As the process continues, headward  
693 erosion can become so strong to break the threshold with a bordering catchment, capturing  
694 part of the neighbouring catchment (Fig. 10, stage b). The capturing river increases the size  
695 of the catchment but the inherited alluvial fan exhibits a small area, compared to the size of  
696 the (enlarged) catchment. At the same time, the captured river has a fan too large compared  
697 to the (reduced) catchment. The capturing river will tend to deliver more sediments,  
698 increasing the size of the alluvial fan in response to the enlarged catchment area (Fig. 10,  
699 stage c). We suggest that the growth/abandonment of fans is similar to the well-established  
700 growth of faults populations, where the growth of nearby fault segments occurs at the  
701 expenses of smaller faults, the offset of which is included into the capturing growing fault  
702 (Kim and Sanderson, 2005).

703

704 Our data indicate a strong correspondence between the most active faults and stream  
705 catchments piracy at the footwall of the normal faults. In the study area, the enhanced faults  
706 activity is further reflected by the active subsidence of the Foligno valley.

707 Since there is nothing peculiar or unique in the fans and faults in the investigated area, we  
708 hypothesize that similar processes occur in similar extensional settings. We conclude that  
709 part of the data scatter commonly observed in fan-area plots may be related to catchments  
710 piracy induced by active tectonics.

711

## 712 **Conclusions**

713

714 We identify the Montefalco ridge in the Northern Apennines as a fossil alluvial-fan which  
715 was dissected by the activation of the NE-dipping Montefalco fault system after Early  
716 Middle-Pleistocene. The Montefalco fan abandonment at the normal faults footwall created a  
717 drainage inversion in which the former river deposit is presently uplifted above the present-  
718 day alluvial plain. The present-day alluvial plain is undergoing active subsidence, triggering  
719 strong headward erosion of the rivers draining into it.

720 We suggest that a change of relative subsidence controlled by the normal faults activity  
721 occurred between the Late Pleistocene and the Holocene. Such distribution positively  
722 correlates with the distribution of the historical seismicity.

723 The river-long profiles draining the Montefalco hill reveal a strong correspondence between  
724 knick-points and the mapped faults. In addition, a knick-point along the Mauro stream in  
725 correspondence of the normal fault closest to the Foligno Valley (Fig. 8c) indicates that the

726 fault displaces a present-day alluvial fan, suggesting that the fault system is active also  
727 during the Holocene. This is also in agreement with the thickening of the alluvial deposits  
728 towards the NE-dipping normal fault observed in the seismic profiles.  
729 Tectonically induced headward erosion caused streams piracy and capture affecting the  
730 dimension of the present-day alluvial fans contributing areas. We plot the alluvial fans areas  
731 vs their contributing areas and find that the data-points follow a regression line in log-log  
732 plot similar to other authors' data-sets. The comparison of the data distribution with the  
733 geomorphological information regarding the river inversions and captures shows that the  
734 rivers which caused piracy at the expenses of other streams have got anomalous large  
735 catchments with respect to their fans dimension and are located below the regression line.  
736 These rivers (capturing) are expected to grow in the size of their fans to equilibrate their  
737 contributing areas. As opposed, the fans of captured rivers are located above the regression  
738 line. Due to the reduction of the size of their catchment area, the captured river is expected  
739 to deliver a reduced amount of sediments to their fans, with the consequent decrease of the  
740 fan growth rate.  
741 We propose a model of alluvial fans growth in active extensional settings in which the  
742 capture of the nearby contributing areas can produce anomalous large values of contributing  
743 areas with respect to the corresponding fan, which has not yet had enough time to re-  
744 equilibrate its volume. The process affects the data-scatter distribution in the alluvial fans  
745 areas/catchment relationships in the study area, and we suggest that the same may occur in  
746 similar extensional settings worldwide. We conclude that stream piracy processes are  
747 sensitive to local rate of tectonic deformation and can contribute to highlight the increase of  
748 activity of individual fault segments in tectonically active areas, benefiting seismic hazard  
749 assessments.  
750 We point out that integrated approaches investigating both the geological record and the  
751 morphotectonics of Quaternary basins, compared with present-day drainage networks, allow  
752 to bridge long-term deformation rates with geodetic rates of deformation, and can help  
753 understand the steadiness/unsteadiness of faults behaviour, unravelling the areas which have  
754 experienced a very recent tectonic perturbation.

755

756

757

### 758 **Acknowledgments**

759 We thank the Editor, P. Hughes, for editorial assistance and two anonymous reviewers for  
760 their constructive and helpful comments.

761

762

### 763 **Funding information**

764 This work was supported by Fondazione Cassa di Risparmio di Perugia, project code  
765 2012.0242021 (grant to F. Mirabella), the Department of Physics and Geology, University of  
766 Perugia (grant to F. Mirabella), the IRPI-CNR (project M3RIGEL, 2016-18), and the Umbria  
767 Region under contract POR-FESR 861.2012.

768

769

### 770 **References**

771 Adamson, K.R., Woodward, J.C., Hughes, P.D., Giglio, F., Del Bianco, F., 2017. Middle  
772 Pleistocene glaciation, alluvial fan development and sea-level changes in the Bay of Kotor,  
773 Montenegro. In: Hughes, P.D., Woodward, J.C. (Eds.) Quaternary glaciation in the  
774 Mediterranean Mountains. *Geological Society of London Special Publications* **433**, 193-209.

775

776 Allmendinger, R.W., Cardozo, N.C., Fisher, D., 2012. *Structural Geology Algorithms:*  
777 *Vectors and Tensors*. England, Cambridge University Press, Cambridge, pp. 289.  
778

779 Alvarez, W. 1999. Drainage on evolving fold-thrust belts: a study of transverse canyons in  
780 the Apennines. *Basin Research* **11**, 267-284.  
781

782 Ambrosetti, P., Carboni, M., Conti, M., Esu, D., Girotti, O., Monica, G. L., Landini, B. &  
783 Parisi, G. 1987. Il Pliocene ed il Pleistocene inferiore del bacino del fiume Tevere  
784 nell'Umbria meridionale. *Geografia Fisica e Dinamica Quaternaria* **10**, 10-33.  
785

786 Ambrosetti, P., Carraro, F., Deiana, G. & Dramis, F. 1982a. Il sollevamento dell'Italia  
787 centrale tra il Pleistocene inferiore e il Pleistocene medio. *CNR Progetto Finalizzato*  
788 *Geodinamica* **513**, 219-223s.  
789

790 Ambrosetti, P., Carraro, F., Deiana, G. & Dramis, F. 1982b. Il sollevamento dell'Italia  
791 centrale tra il Pleistocene inferiore e il Pleistocene medio. Contributo conclusivo per la  
792 realizzazione della Carta Neotettonica d'Italia (II). *CNR Progetto Finalizzato "Geodinamica,*  
793 *S.P. Neotettonica* **356**, 1341-1343.  
794

795 Argenti, P., 2004. Plio-Quaternary mammal fossiliferous sites of Umbria (Central Italy).  
796 *Geologica Romana*, **37**, 67-78.  
797

798 Bally, A., Burbi, L., Cooper, C. & Ghelardoni, R. 1986. Balanced sections and seismic  
799 reflection profiles across the Central Apennines. *Memorie della Società Geologica Italiana*  
800 **35**, 257-310.  
801

802 Barchi, M. 2010. The Neogene-Quaternary evolution of the Northern Apennines: crustal  
803 structure, style of deformation and seismicity. in M. Beltrando, A. Peccerillo, M. Mattei, S.  
804 Conticelli & C. Doglioni, ed., *The Geology of Italy, Journal of Virtual Explorer*.  
805

806 Barchi, M., Brozzetti, F. & Lavecchia, G. 1991. Analisi strutturale e geometrica dei bacini  
807 della media Valle del Tevere e della Valle Umbra. *Bollettino della Società Geologica Italiana*  
808 **110**(8), 65-761.  
809

810 Barchi, M. & Ciaccio, M. 2009. Seismic images of an extensional basin, generated at the

811 hangingwall of a low-angle normal fault: The case of the Sansepolcro basin (Central Italy).  
812 *Tectonophysics* **479**, 285-293.  
813

814 Barchi, M., Feyter, A. D., Magnani, M., Minelli, G., Piali, G. & Sotera, B. 1998.  
815 Extensional tectonics in the Northern Apennines (Italy): evidence from the CROP03 deep  
816 seismic reflection line. *Memorie della Società Geologica Italiana* **52**, 528-538.  
817

818 Barrier, L., Proust, J., Nalpas, T., Robin, C. & Guillocheau, F. 2010. Control of alluvial  
819 sedimentation at Foreland-basin active margins: A case study from the Northeastern Ebro  
820 basin (Southeastern Pyrenees, Spain). *Journal of Sedimentary Research* **80**(8), 728-749.  
821

822 Bartolini, C., D'Agostino, N. & Dramis, F. 2003. Topography, exhumation, and drainage  
823 network evolution of the Apennines. *Episodes* **26**(3), 212-216.  
824

825 Bizzarri, R., Albanelli, A., Argenti, P., Baldanza, A., Colacicchi, R. & Napoleone, G. 2011.  
826 The latest continental filling of Valle Umbra (Tiber basin, central Italy) dated to one million  
827 years ago by magnetostratigraphy. *Il Quaternario* **24**(1), 51-65.  
828

829 Blum, M. & Törnqvist, T. 2000. Fluvial response to climate and sea-level change: a review  
830 and look forward. *Sedimentology* **47**, 2-48.  
831

832 Boncio, P. & Lavecchia, G. 2000. A structural model for active extension in Central Italy.  
833 *Journal of Geodynamics* **29**, 233-244.  
834

835 Bonini, M. 1997. Evoluzione tettonica plio-pleistocenica ed analisi strutturale del bacino  
836 Tiberino e del bacino di Rieti (Appennino umbro-sabino). *Bollettino della Società Geologica  
837 Italiana* **116**, 539-556.  
838

839 Boulton, S. & Whittaker, A. 2009. Quantifying the slip rates, spatial distribution and  
840 evolution of active normal faults from geomorphic analysis: Field examples from an  
841 oblique-extensional graben, southern Turkey. *Geomorphology* **104**, 299-316.  
842

843 Brozzetti, F. & Lavecchia, G. 1995. Evoluzione del campo degli sforzi e storia deformativa  
844 nell'area dei Monti Martani (Umbria). *Bollettino della Società Geologica Italiana* **114**, 155-  
845 176.

846

847 Bucci, F., Cardinali, M. & Guzzetti, F. 2013. Structural Geomorphology, Active Faulting and  
848 Slope Deformations in the Epicenter Area of the 1857 Southern Italy Earthquake. *Physics  
849 and Chemistry of the Earth*, **63**, 12-24.

850

851 Bucci, F., Mirabella, F., Santangelo, M., Cardinali, M. & Guzzetti, F. 2016a, Photo-geology  
852 of the Montefalco Quaternary Basin, Umbria, Central Italy, *Journal of Maps*. DOI:  
853 10.1080/17445647.2016.1210042.

854

855 Bucci, F., Santangelo, M., Cardinali, M., Fiorucci, F. & Guzzetti, F. 2016b. Landslide  
856 distribution and size in response to Quaternary fault activity: the Peloritani Range, NE  
857 Sicily, Italy. *Earth Surface Processes and Landforms*, **41**, 711-720.

858

859 Bull, W. 1991. *Geomorphic Response to Climatic Change*. Oxford University Press, New  
860 York.

861

862 Bull, W. 1977. The alluvial fan environment. *Progress in Physical Geography* **1**, 222-270.

863

864 Buonasorte, G., Cataldi, R., Ceccarelli, A., Costantini, A., DOffizi, S., Lazzarotto, A.,  
865 Ridolfi, A., Baldi, P., Barelli, A., Bertini, G., Bertrami, R., Calamai, A., Cameli, G., Corsi,  
866 R., Dacquino, C., Fiordelisi, A., Ghezzi, A. & Lovari, F. 1988. Ricerca ed esplorazione  
867 nell'area geotermica di Torre Alfina (Lazio – Umbria). *Bollettino della Società Geologica  
868 Italiana* **107**, 265-237.

869

870 Burbank, D. & Anderson, R. 2012. *Tectonic Geomorphology*, 2nd Edition, Wiley-Blackwell  
871 Publishing, Oxford (UK).

872

873 Burbank, D., Meigs, A. & Brozovic, N. 1996. Interactions of growing folds and coeval  
874 depositional systems. *Basin Research* **8**, 199-223.

875

876 Calvache, M., Viseras, C. & Fernandez, J. 1997. Controls on fan development - evidence  
877 from fan morphometry and sedimentology, Sierra Nevada, SE Spain. *Geomorphology* **21**,  
878 69-84.

879

880 Caricchi, C., Aldega, L., Barchi, M., Corrado, S., Grigo, D., Mirabella, F. & Zattin, M. 2015.

881 Exhumation patterns along shallow low-angle normal faults: an example from the  
882 Altotiberina active fault system (Northern Apennines, Italy). *Terra Nova* **27**, 312-321.  
883

884 Cattuto, C., Cencetti, C. & Gregori, L. 1988. Lo studio dei corsi dacqua minori dellItalia  
885 Appenninica come mezzo di indagine sulla tettonica del Plio-Pleistocene. *Bollettino del*  
886 *Museo di Storia Naturale della Lunigiana* **6-7**, 7-10.  
887

888 Cattuto, C. & Gregori, L. 1988. Il colle di Perugia: note di geologia, idrogeologia e  
889 geomorfologia. *Bollettino della Società Geologica Italiana* **107**, 131-140.  
890

891 Cattuto, C., Gregori, L., Melelli, L., Taramelli, A. & Broso, D. 2005. I conoidi  
892 nellevoluzione delle conche intermontane umbre. *Geografia Fisica e Dinamica Quaternaria*  
893 **7**, 89-95.  
894

895 Cencetti, C. 1993. Morfotettonica ed evoluzione Plio-Pleistocenica del paesaggio nellarea  
896 Appenninica compresa tra i monti di Foligno e la Val Nerina (Umbria centro-orientale).  
897 *Bollettino della Società Geologica Italiana* **112**, 235-250.  
898

899 Cencetti, C. 1990. Il Villafranchiano della "riva Umbra" del F. Tevere: elementi di  
900 geomorfologia e di neotettonica. *Bollettino della Società Geologica Italiana* **109**, 337-350.  
901

902 Cencetti, C. 1988. Evoluzione del reticolo idrografico in un tratto Umbro-Marchigiano dello  
903 spartiacque principale dellAppennino. *Geografia Fisisca e Dinamica Quaternaria* **11**(10),  
904 11-24.  
905

906 Chiaraluce, L., Chiarabba, C., Collettini, C., Piccinini, D. & Cocco, M. 2007. Architecture  
907 and Mechanics of an Active Low Angle Normal Fault: the AltoTiberina fault (northern  
908 Apennines, Italy) case study. *Journal of Geophysical Research* **112**, B12399.  
909

910 Ciangherotti, A., Esu, D., 2000. Paleoecologic and biochronologic meaning of the early  
911 Pleistocene molluscan fauna from the Anghiari basin (Tiber River upper valley, central  
912 Italy). *Bollettino della Società Paleontologica Italiana*, **39**(2), 217-224.  
913

914 Cinque, A., Patacca, E., Scandone, P. & Tozzi, M. 1993. Quaternary kinematic evolution of  
915 the Southern Apennines. Relationships between surface geological features and deep



916 lithospheric structures. *Annali di Geofisica* **36**, 249-260.  
917  
918 Colacicchi, R. & Bizzarri R. 2008. Correlation between environmental evolution, historical  
919 settlement and cultural heritage upgrading in Valle Umbra (Central Italy). *Geografia Fisica e*  
920 *Dinamica Quaternaria*. **31**, 107-108.  
921  
922 Collettini, C. & Barchi, M. 2002. A low angle normal fault in the Umbria region (Central  
923 Italy): a mechanical model for the related microseismicity. *Tectonophysics* **359**, 97-115.  
924  
925 Coltorti, M. & Pieruccini, P. 1997. The southeastern Tiber basin (Spoleto, central Italy):  
926 geology and stratigraphy of Plio-Pleistocene sediments. *Il Quaternario* **10**(2), 159-180.  
927  
928 Conti, M. & Girotti, O. 1977. Il villafranchiano nel "lago tiberino", ramo sud-occidentale:  
929 schema stratigrafico e tettonico. *Geologica Romana* **16**, 67-80.  
930  
931 Cowie, P., Attal, M., Tucker, G., Whittaker, A., Naylor, M., Ganast, A. & Roberts, G. 2006.  
932 Investigating the surface process response to fault interaction and linkage using a numerical  
933 modelling approach. *Basin Research* **18**, 231-266.  
934  
935 Cresta, S., Monechi, S. & Parisi, G. 1989. Stratigrafia del Mesozoico e Cenozoico nell'area  
936 umbro-marchigiana. Itinerari geologici sull'Appennino umbro-marchigiano (Italia). *Memorie*  
937 *Descrittive della Carta Geologica d'Italia* **39**, 1-182.  
938  
939 D'Agostino, N., Jackson, J., Dramis, F. & Funiciello, R. 2001. Interactions between mantle  
940 upwelling, drainage evolution and active normal faulting: an example from the central  
941 Apennines (Italy). *Geophysical Journal International* **147**, 475-497.  
942  
943 D'Agostino, N., Mantenuto, S., D'Anastasio, E., Avallone, A., Selvaggi, G., Barchi, M.,  
944 Collettini, C., Radicioni, F., Stoppini, A. & Fastellini, F. 2009. Contemporary crustal  
945 extension in the Umbria-Marche Apennines from regional CGPS networks and comparison  
946 between geodetic and seismic deformation. *Tectonophysics* **476**(1-2), 3-12.  
947  
948 Di Naccio, D., Boncio, P., Brozzetti, F., Pazzaglia, F. & Lavecchia, G. 2013. Morphotectonic  
949 analysis of the Lunigiana and Garfagnana grabens (northern Apennines, Italy): Implications  
950 for active normal faulting. *Geomorphology* **201**, 293-311.

951

952 Doglioni, C., Gueguen, E., Harabaglia, P. & Mongelli, F. 1999. On the origin of west-  
953 directed subduction zones and applications to the western Mediterranean. in B. Durand, L.  
954 Jolivet, F. Horvath & M. Seranne, ed., *The Mediterranean Basins: Tertiary Extension within*  
955 *the Alpine Orogen, Geological Society Special Publications, London*, pp. 541-561.

956

957 Ethridge, F. & Wescott, W. 1984. Tectonic setting, recognition and hydrocarbon reservoir  
958 potential of fan-delta deposits. in E.H. Koster & R.J. Steel, ed., *Sedimentology of Gravels*  
959 *and Conglomerates, Canadian Society of Petroleum Geologists, Memoir*, pp. 217-235.

960

961 Ferrill, D.A., Stakamatos, J.A., Jones, S.M., Rahe, B., McKague, H.L., Martin, R.H. &  
962 Morris, A.P. 1996. Quaternary slip history of the Bare Mountain fault (Nevada) from the  
963 morphology and distribution of alluvial fan deposits. *Geology*, **24**, 559-562.

964

965 Fidolini, F., Ghinassi, M., Magi, M., Papini, M. & Sagri, M. 2013. The Plio-Pleistocene  
966 fluvio-lacustrine Upper Valdarno Basin (central Italy): stratigraphy and Basin fill evolution.  
967 *Italian Journal of Geosciences* **132**, 13-32.

968

969 Fisher, N. I., Lewis, T. L. & Embleton, B. J. 1987. *Statistical analysis of spherical data*.  
970 Cambridge University Press, 329 p.

971

972 Follieri, M. 1977. Evidence on the Plio-Pleistocene palaeofloristic evolution in central Italy.  
973 *Rivista Italiana di Paleontologia e Stratigrafia* **83**, 925-930.

974

975 Frankel, K. & Pazzaglia, F. 2005. Tectonic geomorphology, drainage basin metrics, and  
976 active mountain fronts. *Geografia Fisica e Dinamica Quaternaria* **28**, 7-21.

977

978 Gawthorpe, R. & Leeder, M. 2000. Tectono-sedimentary evolution of active extensional  
979 basins. *Basin Research* **12**, 195-218.

980

981 Ge.Mi.Na. 1962. *Ligniti e torbe dell'Italia centrale*. Geo Mineraria Nazionale, Roma, Italy.

982

983 Gibling, M., Fielding, C. & Sinha, R. 2011. Alluvial fans and alluvial sequences: towards a  
984 geomorphic assessment. *Society for Sedimentary Geology, SEPM Special Publication No.*  
985 **97**, ISBN 978-1-56576-305-0, 423-447.

986

987 Gioia, D., Gallicchio, S., Moretti, M. & Schiattarella, M. 2014. Landscape response to  
988 tectonic and climatic forcing in the foredeep of the southern Apennines, Italy: insights from  
989 Quaternary stratigraphy, quantitative geomorphic analysis, and denudation rate proxies.  
990 *Earth Surface Processes and Landforms*, **39**, 814-835.

991

992 Giraudi, C., Bodrato, G., Ricci Lucchi, M., Cipriani, N., Villa, I.M., Giaccio, B., Zuppi,  
993 G.M. 2011. Middle and Late Pleistocene glaciations in the Campo Felice basin (Central  
994 Apennines – Italy). *Quaternary Research* **75**, 219-230.

995

996 Giraudi, C., Giaccio, B. 2017. Middle Pleistocene glaciations in the Apennines, Italy: new  
997 chronological data and preservation of the glacial record. In: Hughes, P.D. & Woodward,  
998 J.C. (eds) Quaternary Glaciation in the Mediterranean Mountains. *Geological Society*,  
999 *London, Special Publications*, **433**, 161-178.

1000

1001 Gliozzi, E., Abbazzi, L., Argenti, P., Azzaroli, A., Calori, L., Barbato, L. C., Stefano, G. D.,  
1002 Esu, D., Ficcarelli, G., Girotti, O., Kotsakis, T., Masini, E., Mazza, P., Mezzabotta, C.,  
1003 Palombo, M., Petronio, C., Rook, L., Sala, B., Sardella, R., Zanalda, E. & Torre, D. 1997.  
1004 Biochronology of selected mammal molluscs and ostracods from the Middle Pliocene to the  
1005 Late Pleistocene in Italy. The state of the art. *Rivista Italiana di Paleontologia e Stratigrafia*  
1006 **103**(3), 369-388.

1007

1008 Goldsworthy, M. & Jackson, J. 2000. Active normal fault evolution in Greece revealed by  
1009 geomorphology and drainage patterns. *Journal of the Geological Society, London* **157**, 967-  
1010 981.

1011

1012 Gregori, L. 1990. Geomorfologia e neotettonica dell'area di Colfiorito (Umbria). *Geografia*  
1013 *Fisica e Dinamica Quaternaria* **13**, 43-52.

1014

1015 Gregori, L. 1988. Il "bacino di Bastardo": genesi ed evoluzione nel quadro della tettonica  
1016 recente. *Bollettino della Società Geologica Italiana* **107**, 141-151.

1017

1018 Gregori, L. & Cattuto, C. 1986. Elementi geomorfologici ed episodi di tettonica recente nei  
1019 dintorni di Spoleto (Umbria). *Bollettino della Società Geologica Italiana* **105**, 173-184.

1020

- 1021 Guzzetti, F., Marchetti, M. & Reichebach, P. 1997. Large alluvial fans in the north-central Po  
1022 plain (northern Italy). *Geomorphology* **18**, 119-136.
- 1023
- 1024 Harvey, A. 1987. Alluvial fan dissection: relationships between morphology and  
1025 sedimentation. in L. Frostick & I. Reid, ed., *Desert Sediments: Ancient and Modern*,  
1026 *Geological Society, London*, London, UK, pp. 87-103.
- 1027
- 1028 Harvey, A. 2002. The role of base-level change in the dissection of alluvial fans: case studies  
1029 from southeast Spain and Nevada. *Geomorphology* **45**, 67-87.
- 1030
- 1031 Harvey, A., Mather, A. & Stokes, M. 2005. Alluvial Fans: Geomorphology, Sedimentology,  
1032 Dynamics. *Geological Society, London*, London (UK).
- 1033
- 1034 Harvey, A., Wigand, P. & Wells, S. 1999. Response of alluvial fan systems to the Late  
1035 Pleistocene to Holocene climatic transition: contrasts between the margins of pluvial  
1036 Lakes Lahontan and Mojave, Nevada and California, USA. *Catena* **36**, 255-281.
- 1037
- 1038 Hooke, R. 1967. Processes on arid region alluvial fans. *Journal of Geology* **75**, 438-460.
- 1039
- 1040 Hughes, P.D., Woodward, J.C. (Eds.) Quaternary glaciation in the Mediterranean Mountains.  
1041 *Geological Society of London Special Publications* **433**, 193-209.
- 1042
- 1043 Hunstad, I., Selvaggi, G., D'Agostino, N., Clarke, P. & Pierozzi, M. 2003. Geodetic strain in  
1044 peninsular Italy between 1875 and 2001. *Geophysical Research Letters* **30**(4), 1181.
- 1045
- 1046 ISPRA. in press. Foligno, Sheet 324. In: *Carta Geologica d'Italia*, 1:50,000 scale, Roma.
- 1047
- 1048 Jackson, J. & Leeder, M. 1994. Drainage systems and the development of normal faults: an  
1049 example from Pleasant Valley, Nevada. *Journal of Structural Geology* **16**(8), 1041-1059.
- 1050
- 1051 Keller, E. A. 1986. Investigation of active tectonics: Use of surficial Earth processes in  
1052 Active tectonics. Nat.Ac.Press, Washington, 136-147.
- 1053
- 1054 Kim, Y. & Sanderson, D. 2005. The relationship between displacement and length of faults:  
1055 a review. *Earth-Sciences Reviews* **68**, 317-334.

1056

1057 Lavecchia, G., Brozzetti, F., Barchi, M., Keller, J. & Menichetti, M. 1994. Seismotectonic  
1058 zoning in east-central Italy deduced from the analysis of the Neogene to present  
1059 deformations and related stress fields. *Geological Society of America Bulletin* **106**, 1107-  
1060 1120.

1061

1062 Leeder, M. & Gawthorpe, R. 1987. Sedimentary models for extensional tilt-block/half  
1063 graben basins. in M.P. Coward, J.F. Dewey & P.L. Hancock, ed., Continental Extensional  
1064 Tectonics, *Geological Society Special Publications*, London, pp. 139-152.

1065

1066 Lotti, B. 1926. Descrizione geologica dell'Umbria. *Memorie Descrittive della Carta*  
1067 *Geologica d'Italia* **21**, 1-320.

1068

1069 Malinverno, A. & Ryan, B. 1986. Extension in the Tyrrhenian sea and shortening in the  
1070 Apennines as result of arc migration driven by sinking of the lithosphere. *Tectonics* **5**(2),  
1071 227-245.

1072

1073 Marchesini, I., Santangelo, M., Fiorucci, F., Cardinali, M., Rossi, M. & Guzzetti, F. 2013. A  
1074 GIS method for obtaining geologic bedding attitude. in C. Margottini, P. Canuti & K. Sassa,  
1075 ed., *Landslide Science and Practice*, (Vol. **1**), Springer, Berlin, pp. 243-247.

1076

1077 Marrett, R. & Allmendinger, R. 1990. Kinematic analysis of fault-slip data. *Journal of*  
1078 *Structural Geology* **12**(8), 973-986.

1079

1080 Martinetto, E., Bertini, A., Basilici, G., Baldanza, A., Bizzarri, R., Cherin, M., Gentili, S. &  
1081 Pontini, M. 2014. The plant record of the Dunarobba and Pietrafitta sites in the Plio-  
1082 Pleistocene palaeoenvironmental context of central Italy. *Alpine and Mediterranean*  
1083 *Quaternary* **27**(1), 29-72.

1084

1085 Martini, I. & Sagri, M. 1993. Tectono-sedimentary characteristics of Late Miocene-  
1086 Quaternary extensional basins of the Northern Apennines, Italy. *Earth Sciences Reviews* **34**,  
1087 197-233.

1088

1089 Masini, F., Sala, B., 2007. Large and small mammal distribution patterns and  
1090 chronostratigraphic boundaries from the Late Pliocene to the Middle Pleistocene of the

- 1091 Italian peninsula. *Quaternary International*, **160**, 43-56.
- 1092
- 1093 Mather, A., Harvey, A. & Stokes, M. 2000. Quantifying long-term catchment changes of  
1094 alluvial fan systems. *Geological Society of America Bulletin* **112**(12), 1825-1833.
- 1095
- 1096 Mazzanti, R. & Trevisan, L. 1978. Evoluzione della rete idrografica nell'Appennino centro-  
1097 settentrionale. *Geografia Fisica e Dinamica Quaternaria* **1**, 55-62.
- 1098
- 1099 Melelli, L., Pucci, S., Saccucci, L., Mirabella, F., Pazzaglia, F. & Barchi, M. 2014.  
1100 Morphotectonics of the Upper Tiber Valley (Northern Apennines, Italy) through quantitative  
1101 analysis of drainage and landforms. *Rend. Fis. Acc. Lincei*.
- 1102
- 1103 Mirabella, F., Brozzetti, F., Lupattelli, A. & Barchi, M. 2011. Tectonic evolution of a low-  
1104 angle extensional fault system from restored cross-sections in the Northern Apennines  
1105 (Italy). *Tectonics* **30**, TC6002.
- 1106
- 1107 Molin, P., Pazzaglia, F. & Dramis, F. 2004. Geomorphic expression of active tectonics in a  
1108 rapidly-deforming forearc, Sila massif, Calabria, southern Italy. *American Journal of Science*  
1109 **304**, 559-589.
- 1110
- 1111 Pascucci, V., Costantini, A., Martini, I. & Dringoli, R. 2006. Tectono-sedimentary analysis of  
1112 a complex, extensional, Neogene basin formed on thrust-faulted, Northern Apennines  
1113 hinterland: Radicofani basin, Italy. *Sedimentary Geology* **183**, 71-97.
- 1114
- 1115 Pauselli, C., Barchi, M., Federico, C., Magnani, M. & Minelli, G. 2006. The crustal structure  
1116 of the Northern Apennines (central Italy): and insight by the Crop03 seismic line. *American*  
1117 *Journal of Science* **306**, 428-450.
- 1118
- 1119 Pazzaglia, F. 2003. Landscape evolution models. *Development in Quaternary Science* **1**,  
1120 247-274.
- 1121
- 1122 Peters, G. & van Balen, R. 2007. Tectonic geomorphology of the northern Upper Rhine  
1123 graben, Germany. *Global and Planetary Changes* **58**, 310-334.
- 1124
- 1125 Petronio, C., Argenti, P., Caloi, L., Esu, D., Girotti, O., Sardella, R., 2002. Updating

1126 villafranchian mollusc and mammal faunas of Umbria and Latium (Central Italy). *Geologica*  
1127 *Romana*, **36**, 1-24.  
1128

1129 Picotti, V. & Pazzaglia, F. 2008. A new active tectonic model for the construction of the  
1130 Northern Apennines mountain front near Bologna. *Journal of Geophysical Research* **113**,  
1131 B08412.  
1132

1133 Pondrelli, S., Salimbeni, S., Ekstroem, G., Morelli, A., Gasperini, P. & Vannucci, G. 2006.  
1134 The Italian CMT dataset from 1977 to the present. *Physics of the Earth and Planetary*  
1135 *Interiors* **159**(3-4), 286-303.  
1136

1137 Pope, R.J., Hughes, P.D., Skourtsos, E., 2015. Glacial history of Mt Chelmos, Peloponnesus,  
1138 Greece. In: Hughes, P.D., Woodward, J.C. (Eds.) Quaternary glaciation in the Mediterranean  
1139 Mountains. *Geological Society of London Special Publications* **433**, 211-236.  
1140

1141 Pucci, S., Mirabella, F., Pazzaglia, F., Barchi, M., Melelli, L., Tuccimei, P., Soligo, M. &  
1142 Saccucci, L. 2014. Interaction between regional and local tectonic forcing along a complex  
1143 Quaternary extensional basin: Upper Tiber Valley, Northern Apennines, Italy. *Quaternary*  
1144 *Science Reviews* **102**, 111-132.  
1145

1146 QGIS Development Team, 2018. QGIS Geographic Information System. Open Source  
1147 Geospatial Foundation Project. <http://qgis.osgeo.org>.  
1148

1149 Regione Umbria. 2015a. Cartografia geologica e geotematica dell'Umbria 1:10.000 scale.  
1150 <http://www.regione.umbria.it/paesaggio-urbanistica/cartografia-geologica>.  
1151

1152 Regione Umbria. 2015b. Database of geognostic and geophysical surveys.  
1153 [http://storicizzati.territorio.regione.umbria.it/Static/IndaginiGeologicheKmz/Index\\_kmz.htm](http://storicizzati.territorio.regione.umbria.it/Static/IndaginiGeologicheKmz/Index_kmz.htm)  
1154

1155 Ricci Lucchi, F. 1986. The foreland basin system of the Northern Apennines and related  
1156 clastic wedges: a preliminary outline. *Giornale di Geologia* **48**(3), 165-185.  
1157

1158 Ritter, J., Miller, J., Enzel, Y. & Wells, S. 1995. Reconciling the roles of tectonism and  
1159 climate in Quaternary alluvial fan evolution. *Geology* **23**(3), 245-248.  
1160

1161 Roberts, G. 2007. Fault orientation variations along the strike of active normal faults systems

1162 in Italy and Greece: implications for predicting the orientations of subseismic-resolution  
1163 faults in hydrocarbon reservoirs. *American Association of Petroleum Geologists Bulletin*  
1164 **91**(1), 1-20.  
1165

1166 Rook, L., Martinez-Navarro, B. 2010. Villafranchian: The long story of a Plio-Pleistocene  
1167 European large mammal biochronologic unit. *Quaternary International* **219**, 134–144  
1168

1169 Rovida, A., Camassi, R., Gasperini, P. & Stucchi, M. 2011. Catalogo parametric dei  
1170 terremoti italiani CPTI11. Vol. <http://emidius.mi.ingv.it/CPTI>, Istituto Nazionale di Geofisica  
1171 e Vulcanologia, Milano, Italy.  
1172

1173 Santangelo, M., Marchesini, I., Bucci, F., Cardinali, M., Fiorucci, F. & Guzzetti, F. 2015. An  
1174 approach to reduce mapping errors in the production of landslide inventory maps. *Natural*  
1175 *Hazards and Earth System Sciences* **15**(9), 2111-2126.  
1176

1177 Schiattarella, M., Leo, P. D., Beneduce, P., Giano, S. & Martino, C. 2006. Tectonically  
1178 driven exhumation of a young orogen: an example from the Southern Apennines, Italy.  
1179 *Geological Society of America, Special Paper* **398**, 372-387.  
1180

1181 Servizio Geologico d'Italia. 1969. *Carta Geologica d'Italia*, Foglio **131** Foligno. Poligrafica  
1182 e Cartevalori, Ercolano (Na).  
1183

1184 Silva, P., Goy, J., Zazo, C. & Bardaji, T. 2003. Fault-generated mountain fronts in southeast  
1185 Spain: geomorphologic assessment of tectonic and seismic activity. *Geomorphology* **50**, 203-  
1186 225.  
1187

1188 Sorriso-Valvo, M., Antronico, L. & Le Pera, E. 1998. Controls on modern fan morphology in  
1189 Calabria, Southern Italy. *Geomorphology*, **24**, 169-187.  
1190

1191 Stewart, I. & Hancock, P. 1994. Neotectonics, in P.L. Hancock, ed., *Continental*  
1192 *Deformation*. Pergamon Press, Oxford, UK, pp. 370-409.  
1193

1194 Tarquini, S., Isola, I., Favalli, M., Mazzarini, F., Bisson, M., Pareschi, M. & Boschi, E. 2007.  
1195 TINITALY/01: a new Triangular Irregular Network of Italy. *Annals of Geophysics*, **50**(3),  
1196 407-425.



1197

1198 Viseras, C., Calvache, M., Soria, J. & Fernandez, J. 2003. Differential features of alluvial  
1199 fans controlled by tectonic or eustatic accommodation space. Examples from the Betic  
1200 Cordillera, Spain. *Geomorphology* **50**, 181-202.

1201

1202 Yanites, B., Tucker, G., Mueller, K., Chen, Y., Wilcox, T., Huang, S. & Shi, K. 2010. Incision  
1203 and channel morphology across active structures along the Peikang River, central Taiwan:  
1204 Implications for the importance of channel width. *Geological Society of America Bulletin*,  
1205 **122(7/8)**, 1192-1208.

1206

1207 Wegmann, K. & Pazzaglia, F. 2009. Late Quaternary fluvial terraces of the Romagna and  
1208 Marche Apennines, Italy: climatic, lithologic, and tectonic controls on terrace genesis in an  
1209 active orogen. *Quaternary Science Reviews* **28**.

1210

1211 Whittaker, A., Attal, M., Cowie, P., Tucker, G. & Roberts, G. 2008. Decoding temporal and  
1212 spatial patterns of fault uplift using transient river long profiles. *Geomorphology* **100**, 506-  
1213 526.

1214

1215

## 1216 **Figure captions**

1217

1218 **Fig. 1. (a)** Location map of the study area. The map shows the position of the historical  
1219 seismicity ( $M \geq 5$ ), of the main normal faults and the position of the present-day alluvial-fans  
1220 and alluvial deposits. The map also reports a sketch of the underlying geology. **(b)** Study  
1221 area within the main normal faults alignment from Spoleto to the SE to Sansepolcro to the  
1222 NW.

1223

1224 **Fig. 2. (a)** Geological sketch of the area across the Bastardo and Foligno valleys. The sketch  
1225 is oriented SW-NE and is redrawn from- and integrated with- the map after Bucci et al.  
1226 (2016a). The map reports the traces of the high resolution seismic reflection profiles (Fig.5a,  
1227 b) and the trace of the integrated geological cross-section (A-A', Fig.5c). **(b)** Sketch of the  
1228 stratigraphic relationships within the area. See text for stratigraphy details.

1229

1230 **Fig. 3. (a)** View towards the East of the Foligno fan from the Montefalco hill. The rose-  
1231 diagram reports the palaeo-currents indicators of the Montefalco alluvial fan. The diagram is  
1232 the sum (red line) of the data ( $n = 34$ ) acquired by Regione Umbria (2014) (blue line) and of  
1233 the data ( $n = 32$ ) within this work (green line). Inset a) also reports the position of the  
1234 outcrops of insets 3c and 3d.

1235 **(b)** Example of embriate clasts in the Montefalco Unit composed of organised in layers.

1236 The stereographic projection reports the poles ( $n = 28$ ) of bedding layers (yellow), the dip  
1237 direction (blue) of embriate planes ( $n = 32$ ), and the computed flow direction (blue arrow).

1238 **(c)** Well cemented embriate clasts of the Montefalco Unit. The position of the outcrop is  
1239 Fig. 3a). **(d)** Outcrop of the Montefalco Unit at Foligno (outcrop position in Fig. 3a). Here,  
1240 the facies is more proximal than at Montefalco ( Figs. 3b and 3c).

1241

1242 **Fig. 4. (a)** View towards the South of the Montefalco hill, showing the sub-horizontal beds  
1243 (yellow) and the morphological evidence of the NE-dipping normal faults. The stereo-plot is  
1244 the stereographic projection (Schmidt net, lower hemisphere) of the mapped normal faults ( $n$   
1245  $= 7$ ) and the resulting stresses analysis. **(b)** Outcrop of a normal fault ( position in a) within  
1246 the continental sequence and fault kinematics. **(c)** View of the western part of the Bastardo  
1247 valley (filled by the Colle del Marchese Unit – CU, and the Bevagna Unit - BU), at the  
1248 contact with the Mt. Martani ridge (shaped on the Bedrock). The stereographic projection  
1249 (Schmidt net, lower hemisphere) reports poles to planes ( $n = 27$ ) of the Giano dell'Umbria  
1250 Fault system and the resulting average dip and kinematics (red arrow). **(d)** Geometry and  
1251 kinematics of one of the faults of the Giano dell'Umbria fault System (position in c)

1252

1253 **Fig. 5. (a-b)** High resolution seismic reflection profiles (trace in figure 2a) showing the  
1254 depth geometry of the Bevagna Unit, of the normal faults bordering the eastern flank of the  
1255 Montefalco hill and the thickness of the alluvial deposits. **(a)** Shows the difference in seismic  
1256 facies between the bedrock at the normal faults footwall and the layered continental  
1257 sequence made of sands and clays. **(b)** SW-tilt of the Bevagna Unit and alluvial deposits  
1258 thickening towards the SW. **(c)** Geological cross-section (trace in figure 2) across the  
1259 Foligno valley which integrates the surface geology and the seismic profiles of a) and b).  
1260 The SW part of the section is extrapolated to depth of the basis of a) and b), the NE part of  
1261 the section is extrapolated to depth on the basis of previous work (Barchi et al., 1991). The  
1262 section reaches the outcrop of the Montefalco Unit near Foligno (locality "I Cappuccini",  
1263 Fig.2a).

1264

1265 **Fig. 6.** Geomorphological map of the study area. The map is oriented E-W and shows the  
1266 evidences of drainage perturbation on both the western and eastern reliefs induced by the  
1267 increase in subsidence of the Foligno valley. The numbers refer to the drainage areas of  
1268 specific rivers which captured or were captured by a nearby river. The numbers are the same  
1269 as those in figure 7. We mapped the geomorphological anomalies related to the migration of  
1270 the watershed, hanging palaeo-valleys, anomalous confluences and the direction of the  
1271 palaeo-rivers for the most significant rivers in the study area. See text for description and  
1272 discussion.

1273

1274 **Fig. 7. (a)** Log-Log plot of the alluvial fans areas towards basins areas of the study area. The  
1275 regression line was obtained through a logarithmic space quantile regression, applied to the  
1276 50<sup>th</sup> (dotted thick line) 5<sup>th</sup>, and 95<sup>th</sup> percentiles (grey shaded area) of the distribution. The  
1277 data distribution is self-similar (equation of the type  $A_F = q * A_B^n$ ). **(b)** Distribution of the  
1278 alluvial fans (points in Figure 7a) related to capturing and captured rivers. In both figures,  
1279 red and black numbered circles represent the alluvial fans related to rivers clearly perturbed  
1280 by the Foligno valley subsidence which induced captures and drainage inversions (Figure 6).

1281

1282 **Fig. 8. (a)** stream-long profiles of the Mauro, La Fornace and La Torre streams plotted  
1283 together with the downstream variation in slope % ( $dH/dL$ , where H is elevation and L is  
1284 distance). The symbols (diamond, circle, triangle, square and star) represent the  
1285 correspondence between stream knick-points and mapped normal faults. **(b)** map location  
1286 (inset of in Fig. 2) of the streams shown in a) on the NE-flank of the Montefalco hill. **(c)**  
1287 drape of an aerial photograph on a 10m resolution DEM (TIN-Italy - Tarquini et al., 2007).  
1288 We used a three-times vertical exaggeration to mimic the vertical exaggeration of the  
1289 stereoscopic images. The image was drawn by using the QGIS2threejs plugin of QGIS  
1290 (QGIS Development Team, 2018). On the image, the trace of the normal fault affecting the  
1291 Holocene alluvial fans is evidenced with the white arrows.

1292

1293 **Fig. 9.** Tectono-sedimentary evolution of the study area. (a) Early-Middle Pleistocene, initial  
1294 formation of the continental basin. (b) Middle-Late Pleistocene, the increase in activity of  
1295 the Montefalco east-dipping fault downthrows the Foligno valley and uplifts the Montefalco  
1296 fan (c) Upper Pleistocene-Holocene, further downthrowing of the Foligno valley and strong  
1297 stream headward erosion. See text for details.

1298

1299 **Fig. 10.** Conceptual sketch of the growth of a set of alluvial fans in an actively subsiding  
1300 basin where one or more fault segments are more active than others. Increase of tectonic  
1301 subsidence triggers headward erosion and drainage capture of neighboring rivers. See text  
1302 for explanation.

1303

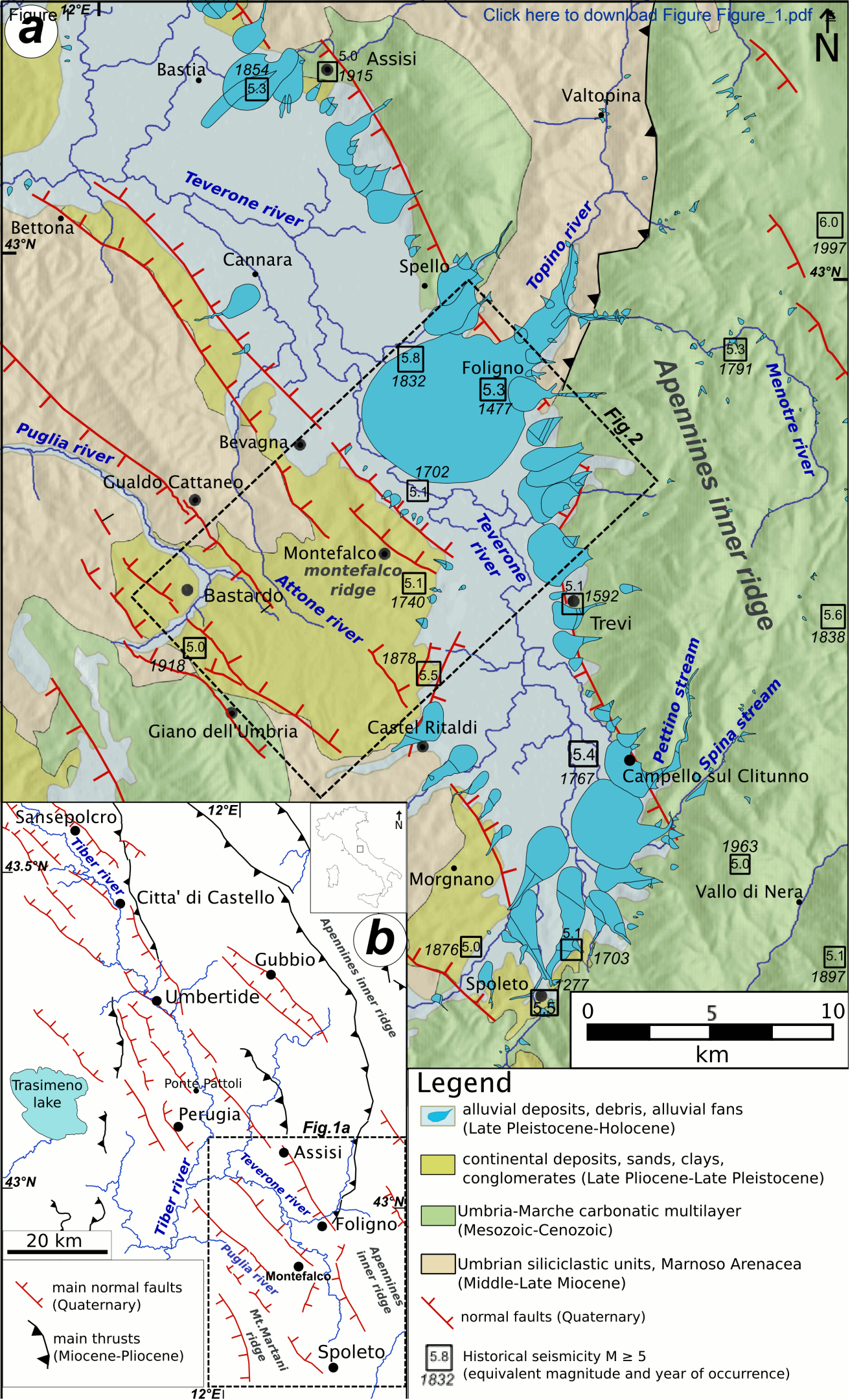
1304

1305 **Table caption**

1306

1307 **Table 1.** Stratigraphical, depositional and tectonic features of the continental deposits of the  
1308 study area. See text for details.

<i>Lithostratigraphic Unit</i>	<i>Stratigraphic feature</i>	<i>Depositional environment</i>	<i>Age</i>	<i>Evidences of tectonic activity</i>
Alluvial deposits (AD)	Fine-grained floodplain sediments made of gray and yellowish clays and sandy clays	Floodplain	Late Pleistocene - Holocene	Thickening at the fault hanging-wall at the base of the E slope of the Montefalco Hill
Alluvial fans (AF)	Coarse-grained fan-shape debris deposits in a silt and subordinately clay matrix	Alluvial, fluvial	Late Pleistocene - Holocene	Fans aligned at the hanging-wall of the Foligno Valley bounding faults
Pianacce Unit (PU)	Brown and subordinately red clay and silty clay with sporadic carbonate clasts	Palustrine, locally connected to distal part of alluvial fan environment	Middle - Late Pleistocene	The deposit is present only in the Bastardo valley with no direct evidence of faulting
Colle del Marchese Unit (CU)	Conglomerate and gravel made up of clasts of mesozoic-cenozoic carbonates, in a silt and subordinately clay matrix	Poor rounding of pebbles indicates a fluvial depositional environment proximal to the origin	Early-Middle Pleistocene	Faulted deposits at the hanging-wall of the Giano dell'Umbria fault System (Mt. Martani ridge)
Montefalco Unit (MU)	Conglomerate and gravel made up of rounded locally sub-angular and rarely flat pebbles and cobbles in a sand or silt matrix. Clasts are Mesozoic-Cenozoic carbonates and subordinately sandstones of E-NE origin.	Gravel bar deposition alternated to sandy and silty layers suggests a braided pattern in the middle and distal part of alluvial fan environment	Early-Middle Pleistocene	i) Faulted deposits ii) Evidence of fault escarpment locally marked by triangular facets iii) Deposit uplifted at the footwall of the active fault system bounding SW the Foligno Valley
Bevagna Unit (BU)	Grey and yellow clay, sandy-clay with minor conglomerate lenses. Lignite layers are present locally.	Fine sediment related to floodplain, lacustrine or shallow lake environment	Early Pleistocene	i) Faulted deposits ii) Inclined and tilted bedding related to fault activity



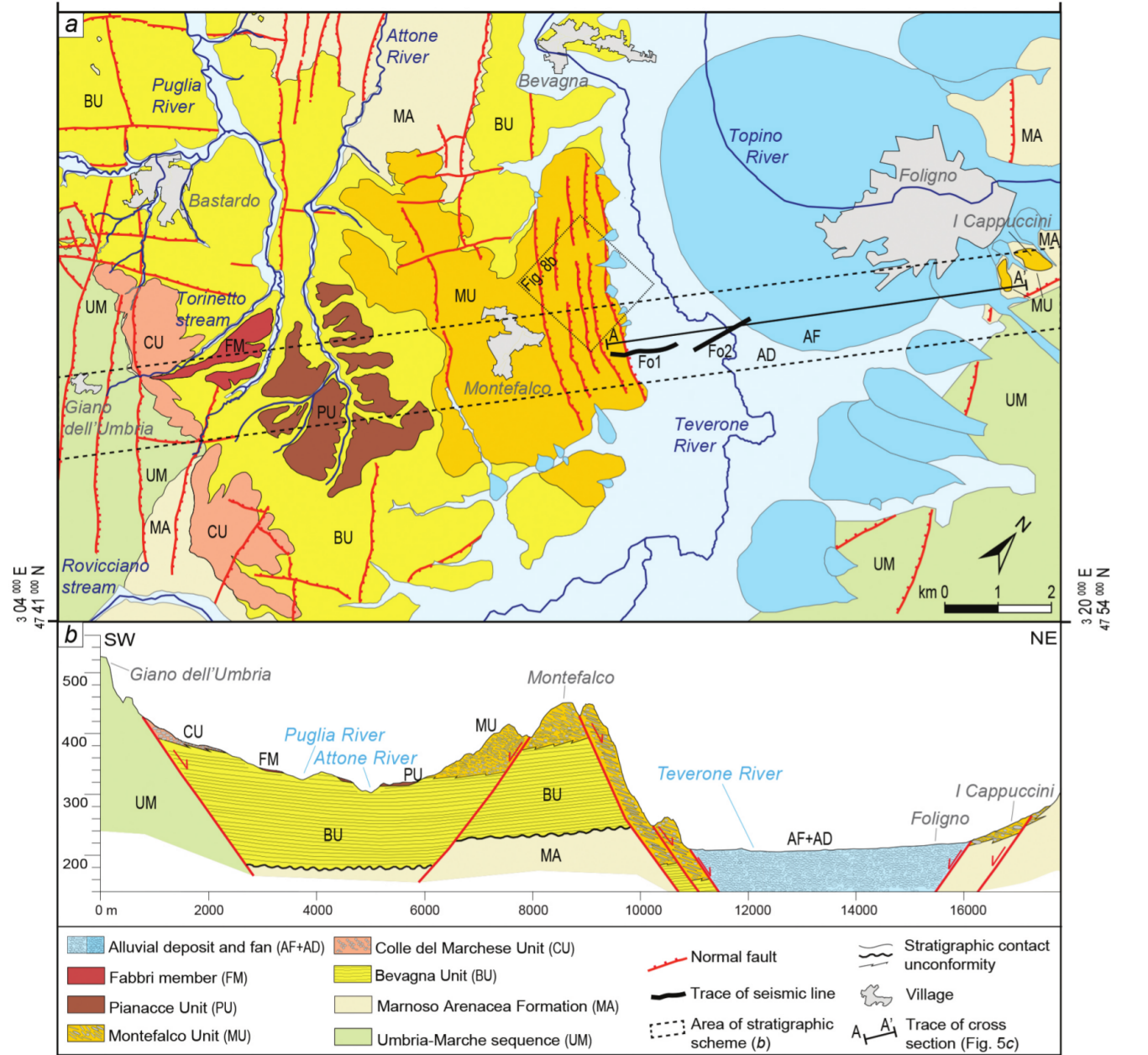
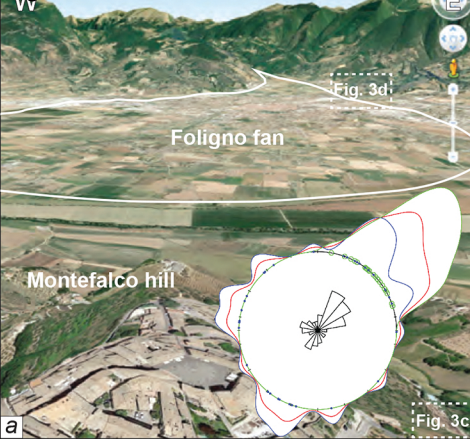


Figure 3



Click here to download Figure  
figure\_3.pdf

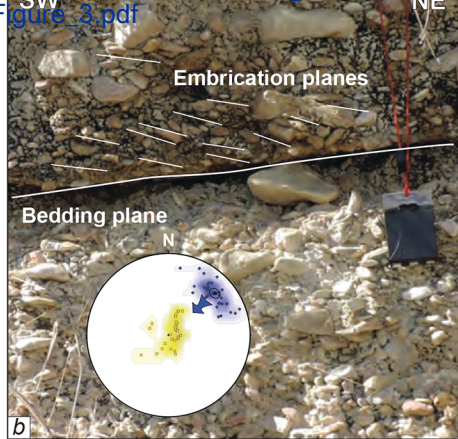
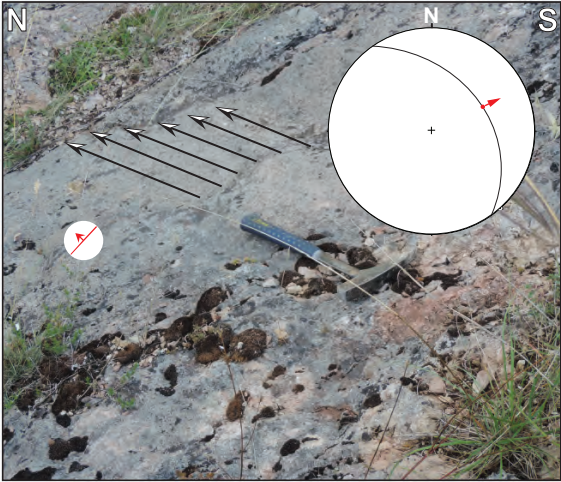
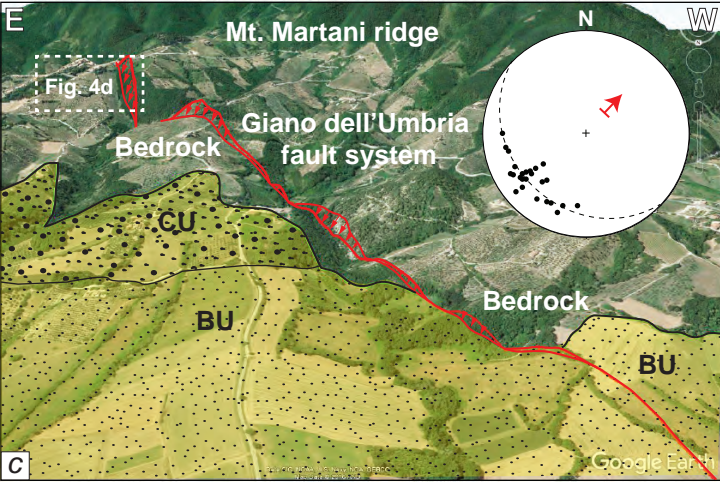
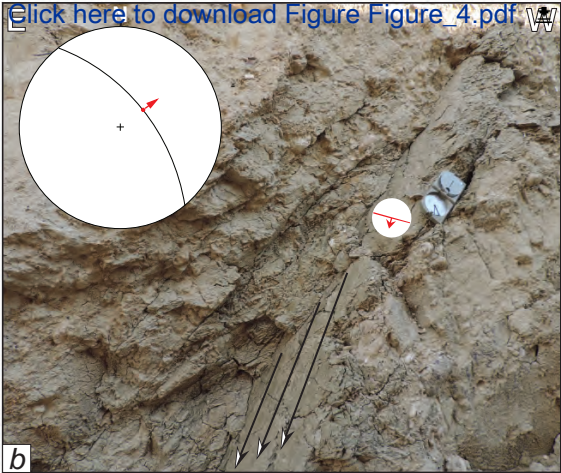
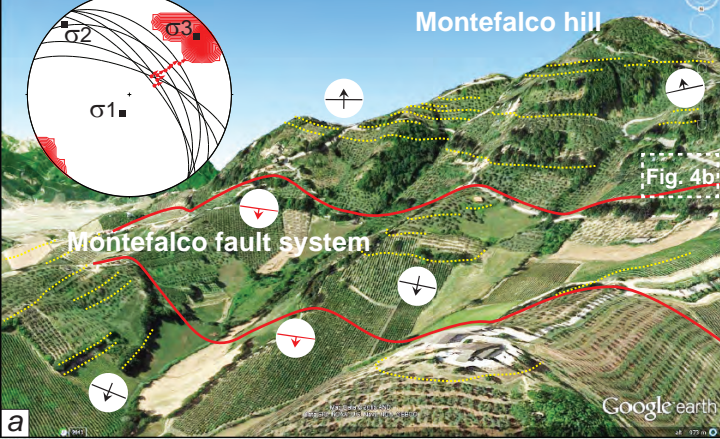
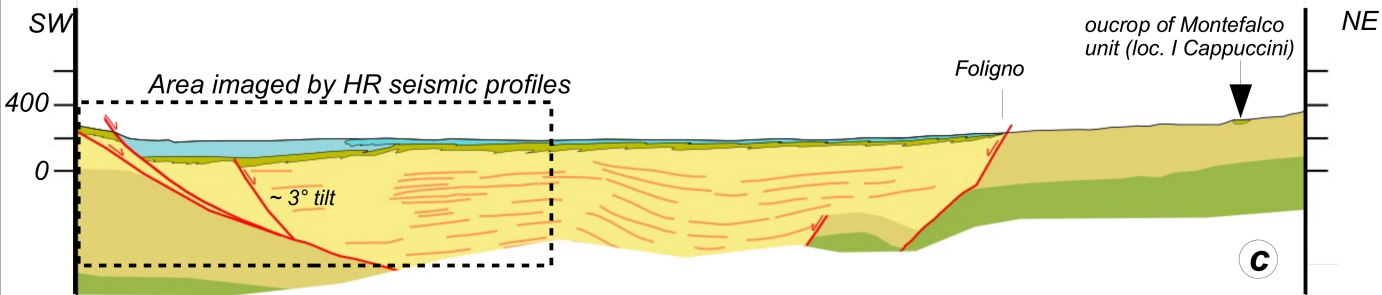
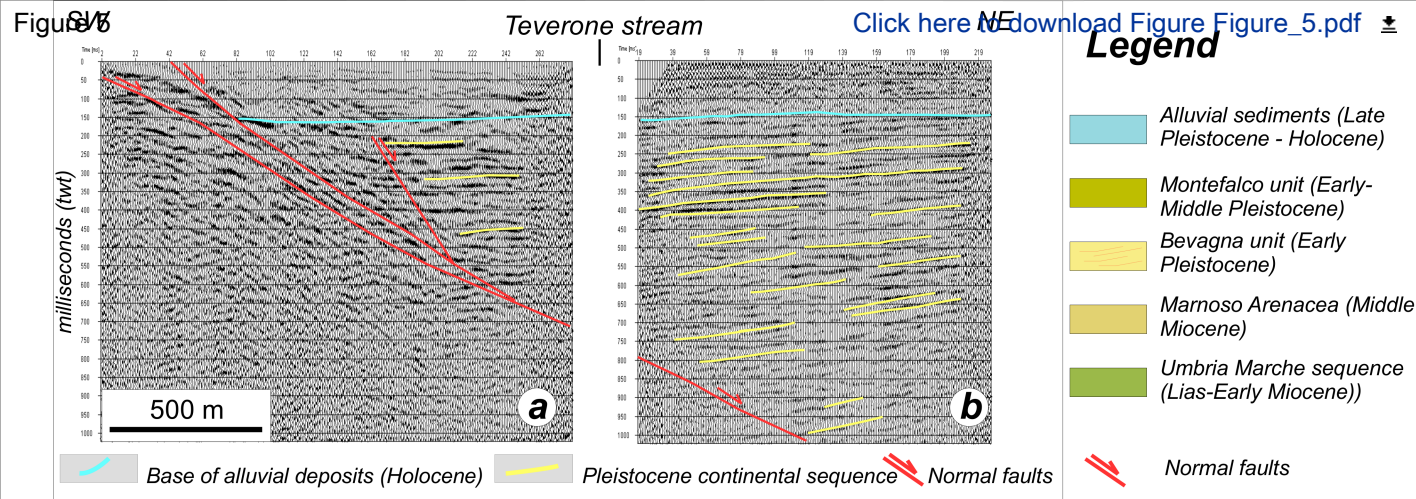


Figure 4



[Click here to download Figure Figure\\_4.pdf](#)





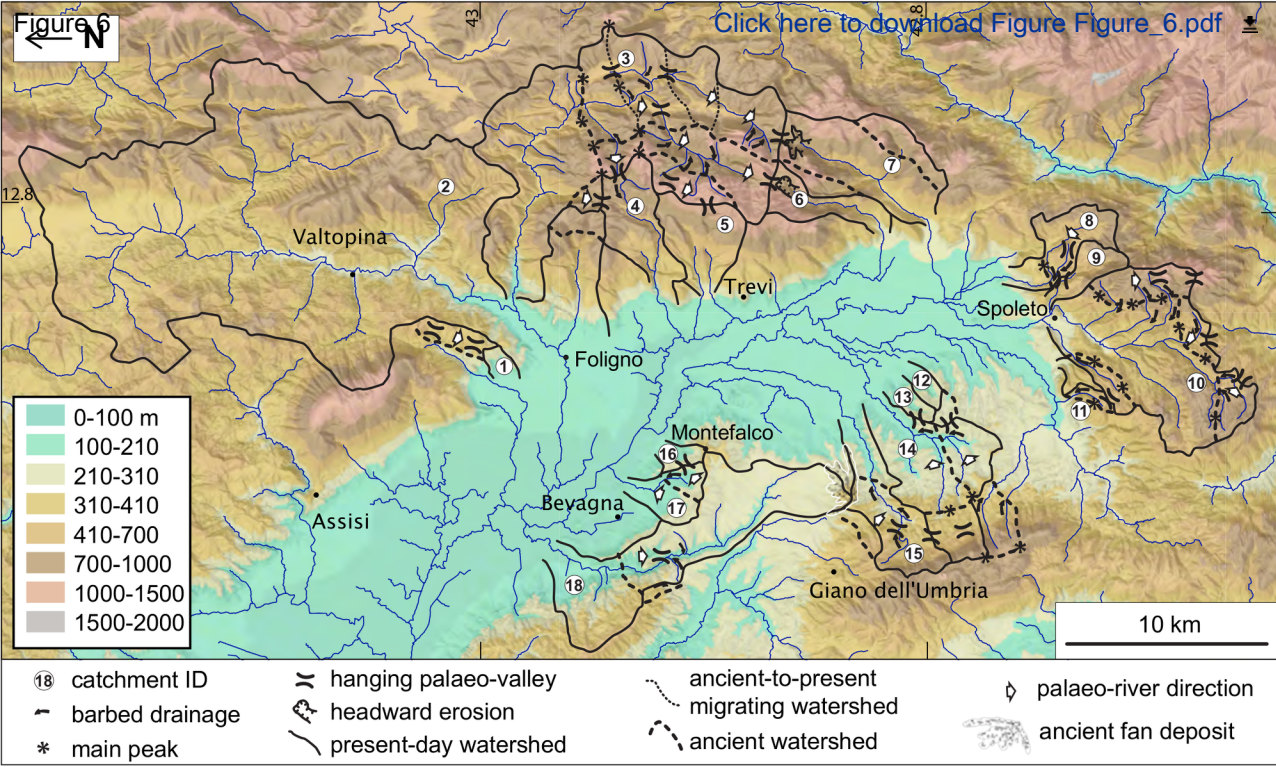


Figure 7

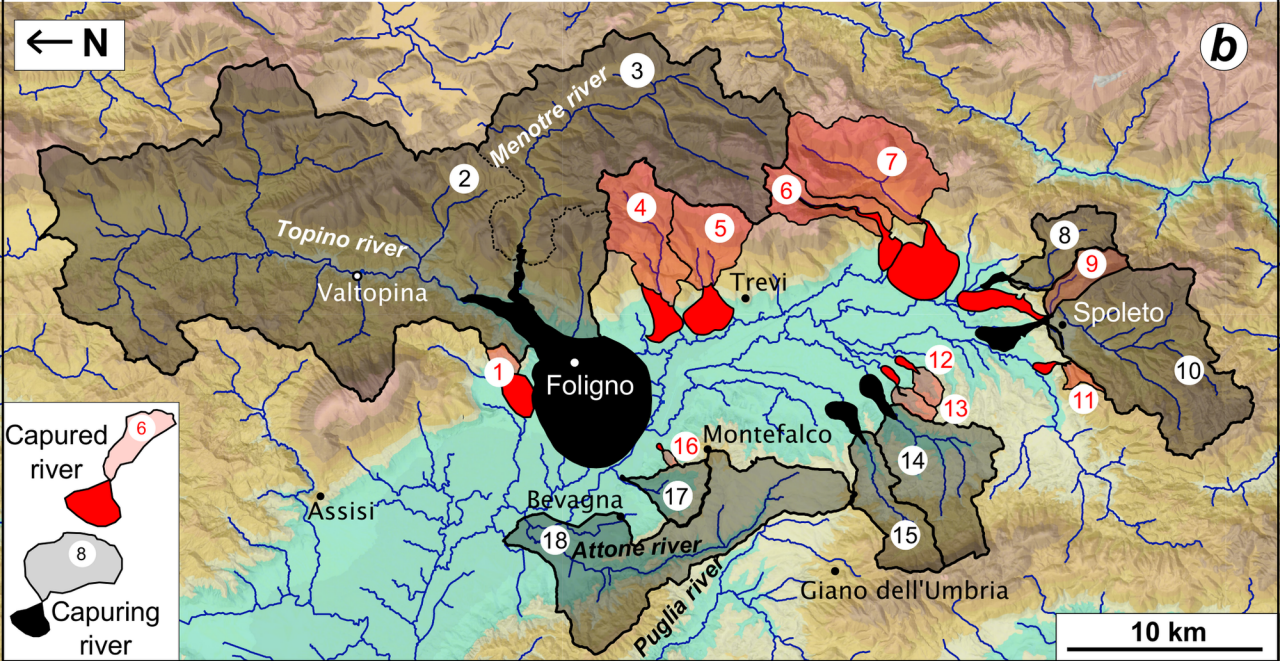
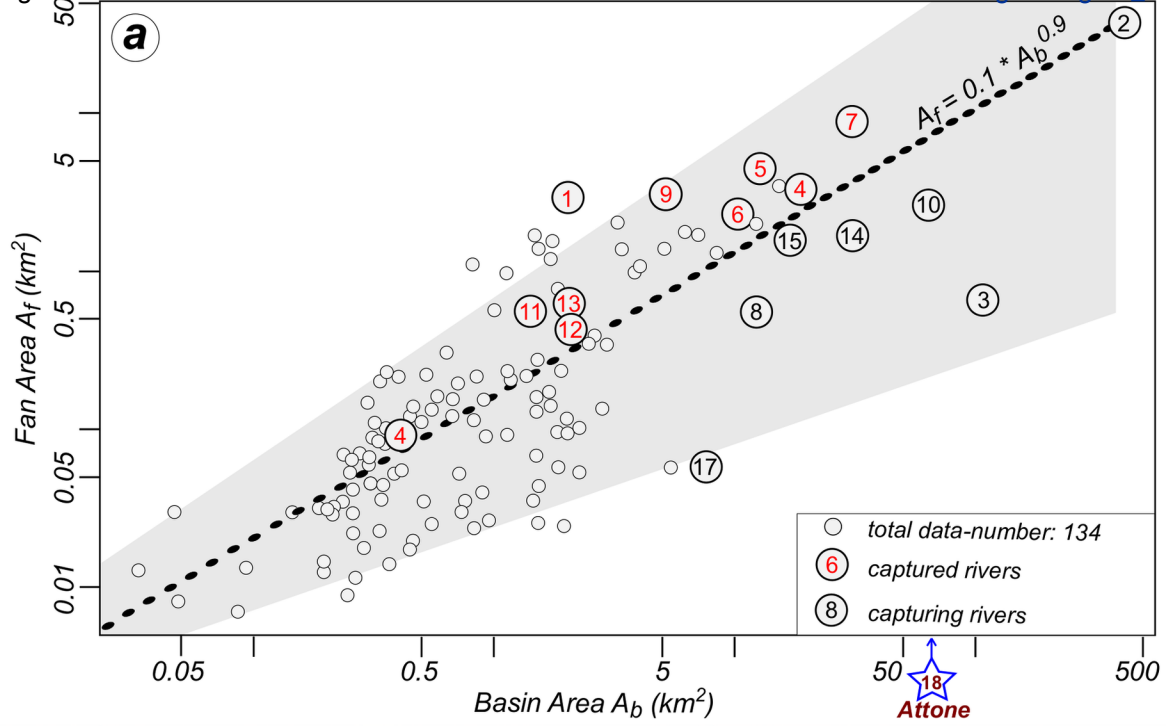


Figure 8

[Click here to download Figure Figure\\_8.pdf](#)

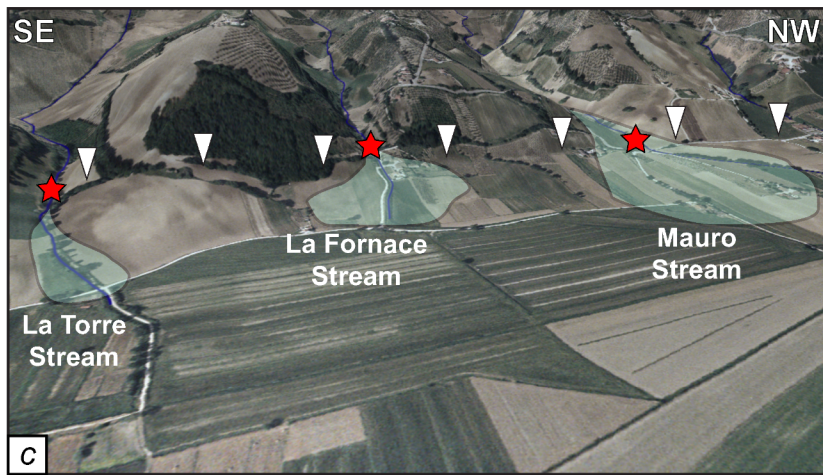
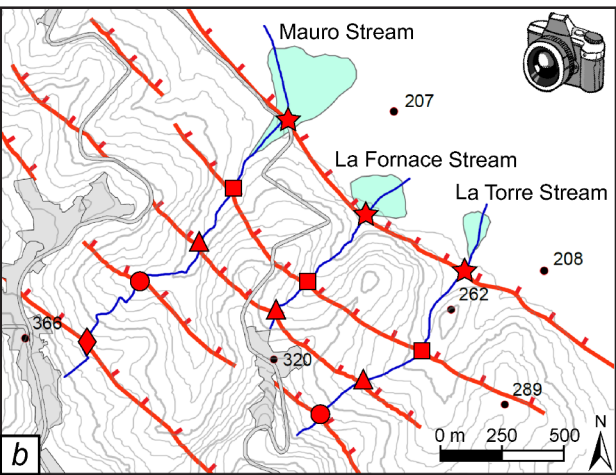
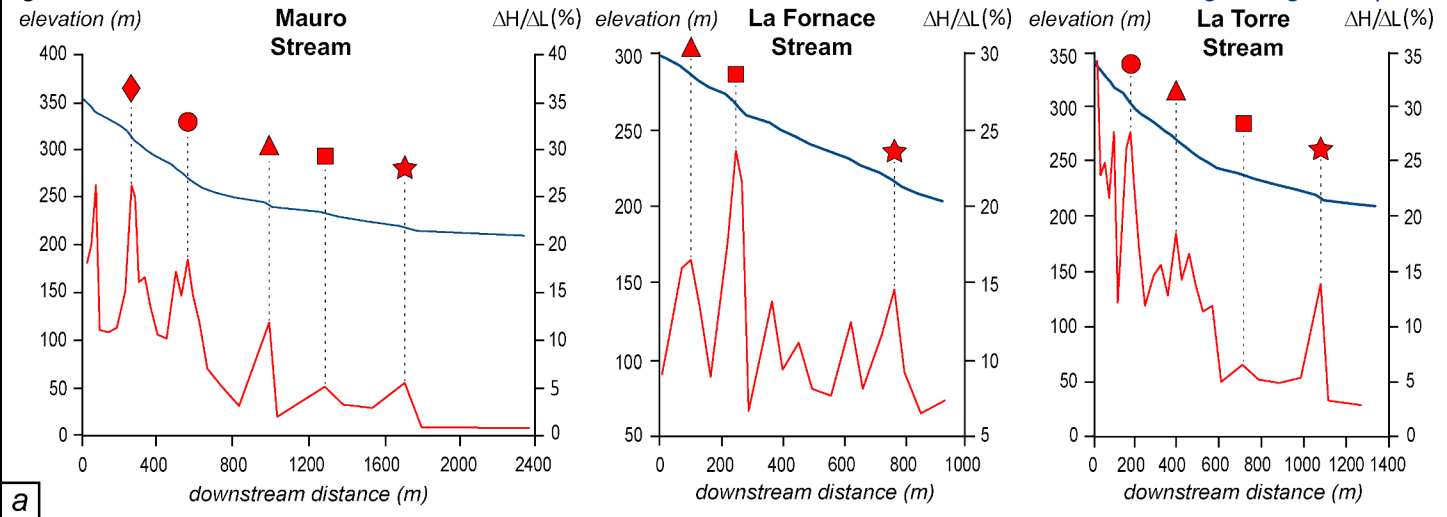
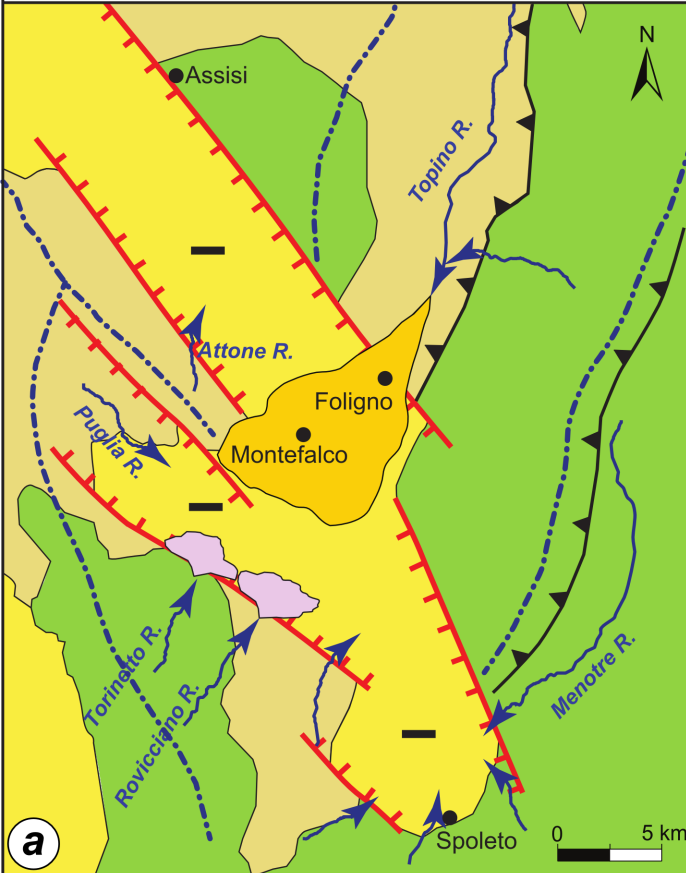
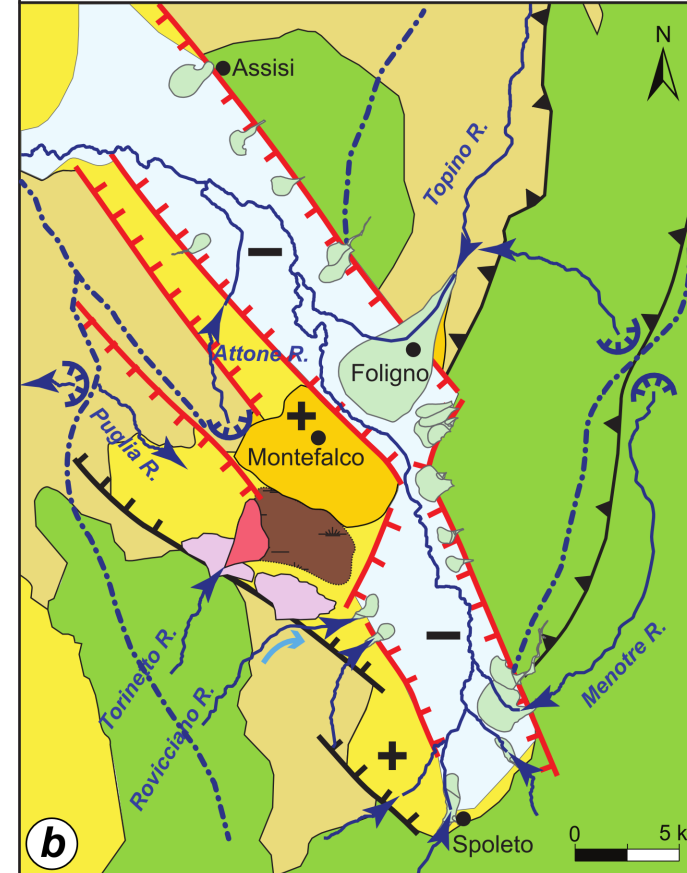


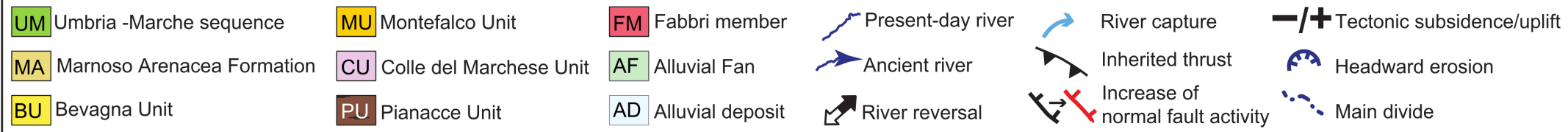
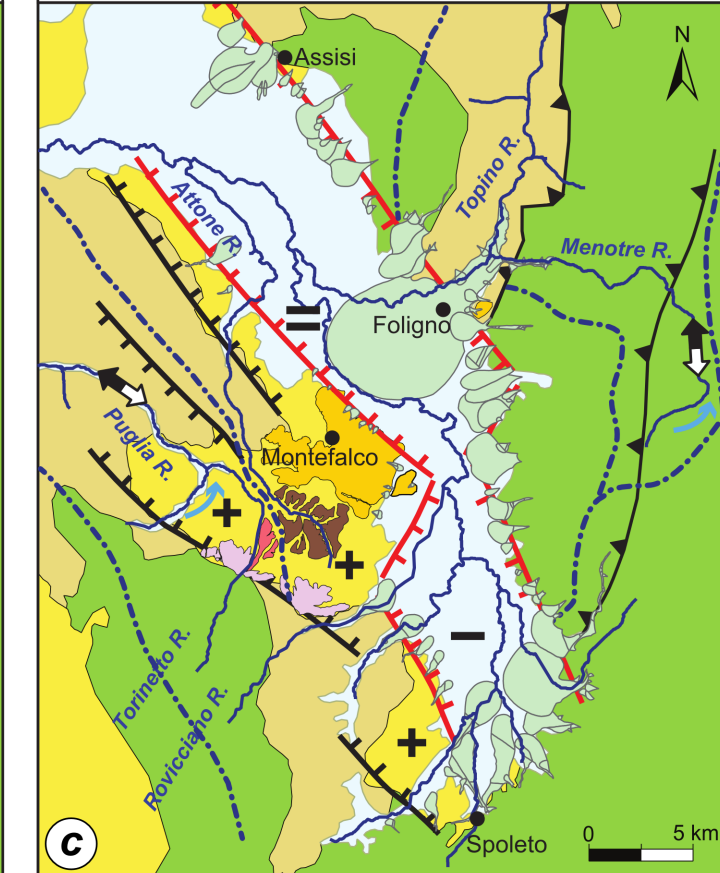
Figure 9 Early-Middle Pleistocene



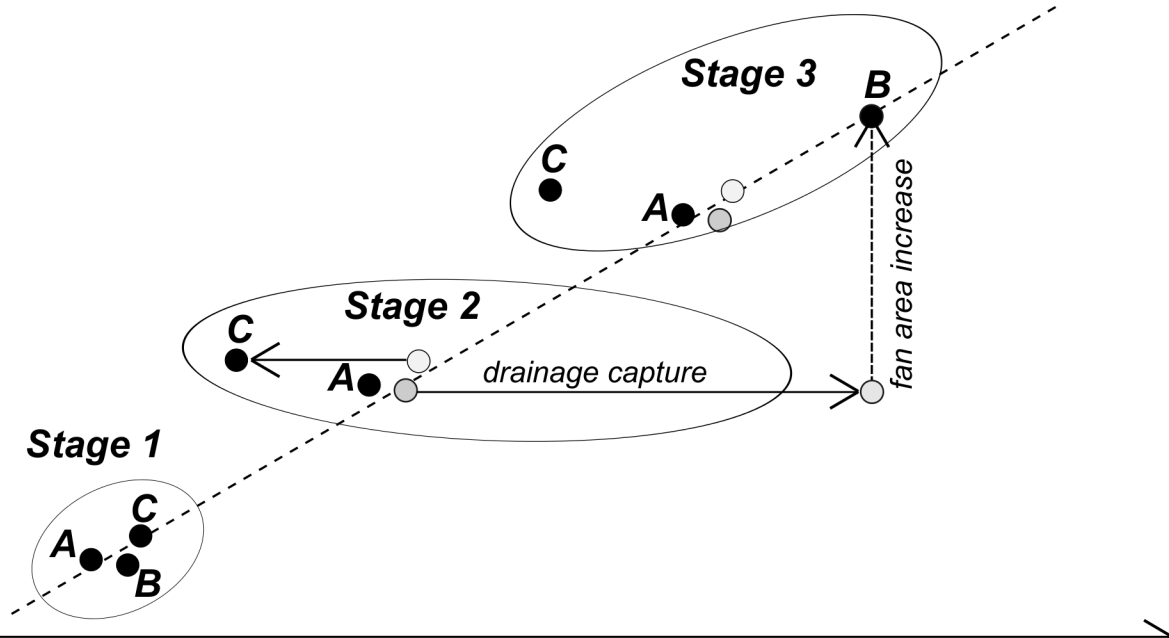
Middle-Late Pleistocene



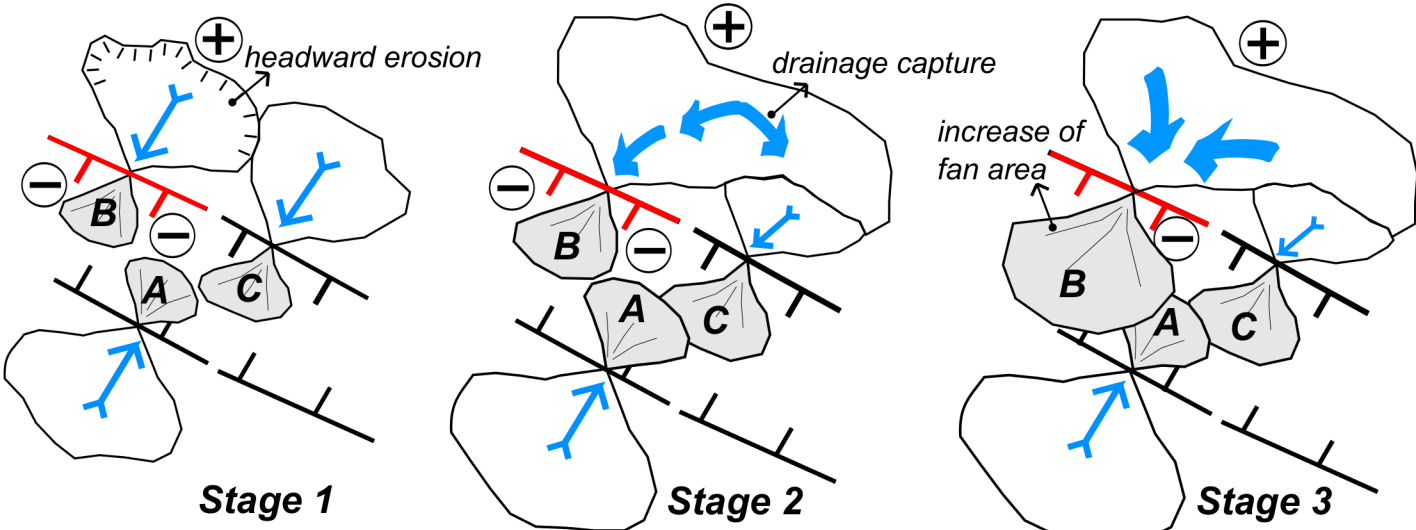
Climate transition to Present



Log (Fan area)

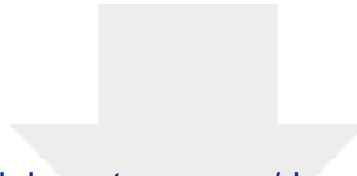


Log (Basin area)



+ uplift increase   - subsidence increase

not to scale



[Click here to access/download](#)

**Supplementary material (not datasets)**

[jgs2017\\_138\\_revised\\_21May\\_2018\\_changes.pdf](#)

